Hydrochar from Hydrothermal Liquefaction of Spent Coffee Grounds for Cementitious Composites: Effects on Strength, Porosity, and Carbon Footprint

Alireza Jafari[1,*] and Pedram Sadeghian[2]

[1] *Ph.D. Candidate in Civil Engineering, Department of Civil and Resource Engineering, Dalhousie University, Halifax, Nova Scotia, B3H 4R2, Canada. E-mail: Alireza.Jafari@dal.ca*

[2] *Associate Professor and Canada Research Chair in Sustainable Infrastructure, Department of Civil and Resource Engineering, Dalhousie University, Halifax, Nova Scotia, B3H 4R2, Canada. E-mail: Pedram.Sadeghian@dal.ca*

* *Corresponding author*

Abstract

This study examines the effect of hydrochar from hydrothermal liquefaction (HTL) of spent coffee grounds on the compressive strength (CS), unit weight (UW), ultrasonic pulse velocity (UPV), microstructure, and carbon footprint of mortars at 0–2.5% dosages. Compared to hydrochar from hydrothermal carbonization (HTC), HTL-derived hydrochar has a higher carbonization and lower wooden organics, making it a promising low-carbon solution for cementitious composites. However, its performance in the composites has not been explored. A total of 63 mortar specimens were prepared and tested at 7, 28, and 90 days. Results showed that hydrochar increased porosity at all ages, leading to reductions of 7.91% and 13.09% in 90-day UW and UPV, respectively. Its effect on CS was age-dependent; at 7 days, incorporating 0.5% hydrochar as an additive and SCM increased CS by 59.60% and 19.23%, respectively. However, higher dosages negatively impacted hydration due to the high-water retention capacity of hydrochar. At 28 days, hydrochar-containing specimens achieved higher CS than reference specimens, reaching peak performance. By 90 days, acidity, porosity, deterioration, and low reactivity of hydrochar, along with the negative effects of accelerated hydration, reduced CS by 21.33% (SCM) and 14.12% (additive) at a 2.5% dosage.

Using 0.5% hydrochar as an additive was the most effective approach, enhancing CS at 7 and 28 days and reducing the composite's carbon footprint by 1.15% with minimal impact on 90-day CS (<1%). Carbon sequestration analysis showed 1 kg of hydrochar captures 1.502 kg CO_2-eq, reducing emissions by up to 8.09% at 2.5% replacement.

DOI: https://doi.org/10.1016/j.conbuildmat.2025.141134

Keywords: Hydrochar, Additive, Cement replacement, Compressive strength, Microstructure, Porosity, Carbon footprint

1. Introduction

Rapid population growth in recent decades has boosted urbanization, surging the demand for new infrastructures and construction materials, particularly concrete. Increasing the concrete supply raised the need for one of the most environmentally unfriendly construction materials, ordinary Portland cement (OPC). Earlier studies [1,2] estimated that OPC accounts for 8% and 6% of annual global carbon dioxide (CO_2) and greenhouse gas emissions, respectively. This substantial environmental impact and the critical state of global climate change emphasize the pressing demand for reducing the portion of OPC in cementitious composites, addressed by replacing it with supplementary cementitious materials (SCMs) [3,4]. The technique also lessens the burden on natural resources since producing each ton of OPC needs 1.5 tons of raw materials [5].

Biomass is a potential SCM that was used to reduce the demand for OPC in cementitious composites [6,7]. Despite the environmental benefits of using biomass as an SCM, its features adversely affect the properties of cementitious composites by increasing porosity, promoting microcracking, and hindering hydration reactions [7]. Accordingly, advanced techniques were required to reduce the organic structures of biomass prior to its reuse in the composites.

Traditionally, direct combustion was used in power plants to produce energy, which converts biomass into SCM-usable ashes. However, given the environmental impacts of direct combustion, recent environmental regulations attempt to limit this practice and replace it with eco-friendly thermal decomposition techniques, i.e., pyrolysis and hydrolysis.

Pyrolysis involves the thermal decomposition of biomass in low-oxygen chambers, producing syngas and biochar. The syngas is used as a power source while the biochar is the byproduct. An earlier study [8] showed that pyrolysis could reduce the CO_2 emissions from power generation plants by 67% compared to the traditional technique. Given these environmental advantages and the need for reusing biochar, earlier studies [9–11] examined the effect of replacing OPC with biochar on the properties of cementitious composites. Their results [10,11] indicated that biochar could significantly enhance the early-age hydration and carbonization of surrounding cement paste by increasing the compactness of the fresh mix, providing retained water and nucleation sites for accelerating hydration, and offering dissolved carbon for early carbonization. Belaadi et al. [12] demonstrated that increasing the pyrolysis temperature from 300 to 500°C enhances the mechanical strength of biochar-modified cementitious mortars within the first 28 days by affecting the biochar's physicochemical properties. Despite this potential, a few studies [10,13] raised concerns about the durability of biochar-modified composites. The exposure of biochar to cement paste could deteriorate biochar, which released fulvic acid into the cement paste and weakened the structure of biochar and nearby cement paste over time.

Besides pyrolysis, the application of hydrothermal decomposition to produce energy has recently gained significant attention. Hydrothermal decomposition is a chemical process in which biomass is exposed to hot-compressed water to produce biofuel or carbon-rich solids. This process can be categorized into three classes based on the operation temperature: 1) hydrothermal carbonization, HTC, (ranging from 180 to 250 °C), 2) hydrothermal liquefaction, HTL, (ranging from 250 to 375 °C), and 3) hydrothermal gasification (above 375 °C) [14]. According to Lachos-Perez et al. [15], the HTC produces solid fuel (hydrochar), which can be combusted as a coal substitute or used to extract bio oil with further processing. However, HTL could directly produce biocrude oil, which can be refined as biofuel and used as a sustainable fossil fuel alternative. Consequently, although HTC consumes lower energy and thereby emits less CO_2 than HTL, HTL has higher efficiency and lower energy consumption in producing biofuel. Moreover, the hydrochar is the main product of HTC, while it is the byproduct of HTL.

Comparing pyrolysis and hydrolysis indicated that the lack of demand for drying biomass and the decreased operating temperature in hydrothermal decomposition could significantly reduce the energy consumption of hydrolysis relative to pyrolysis [15]. Quantitatively, producing each kilogram of bio-oil by HTL and pyrolysis could release 3.55 kg and 8.27 kg of CO2, respectively [16]. Despite the associated environmental benefits, incorporating hydrothermal decomposition methods presents challenges in water-scarce regions due to their high water demand. According to this challenge, it could be expected that using HTL is likely to increase in coastal regions, which raises the need to develop a valuable application for its primary byproduct, hydrochar.

Considering the similarities in physicochemical properties between hydrochar and biochar, hydrochar may serve as an SCM in cementitious composites. Incorporating hydrochar in cementitious composites may enhance the composite's properties, decrease the demand for ordinary Portland cement (OPC), and provide a sustainable waste management solution for hydrochar. Additionally, the carbon sequestration potential of hydrochar may mitigate the carbon footprint associated with the composite. Despite its potential, to the authors’ knowledge, the effect of using hydrochar derived from HTL on the properties of cementitious composites has not been examined by scholars.

Recent studies investigated the effect of hydrochar derived from HTC on mortar properties [17,18] . Santos et al. [17] examined the effect of incorporating hydrochar derived from the HTC of rice husks and stabilized organic fractions on the properties of cementitious mortars. They [17] conducted HTC at 200°C for 2 hours under a pressure of 16 bars. The researchers processed the hydrochar through grinding and sieving to obtain particles with dimensions less than 100 μm. Their results demonstrated that substituting OPC with hydrochar at a range of 1.25% to 5% decreased the mechanical strength of the mortars by up to 60% at 7 days. However, the specimens containing hydrochar demonstrated significant strength development from 7 to 28 days, achieving up to 74% of the strength of reference specimens at 28 days.

Sharma et al. [18] assessed the effect of adding hydrochar derived from pomegranate peel at 0.1%, 0.25%, 0.5%, and 1% dosages on the mechanical properties of cementitious mortars. The study involved conducting HTC at 250°C for 4 hours to produce hydrochar. The researchers then examined the effect of hydrochar dosage and wet and dry mixing methods on the mechanical strength of mortar. Their data indicated that the effect of hydrochar dosage on the compressive strength of the specimens was more significant than that of the mixing technique. The findings also presented that reusing hydrochar from HTC decreased the CS of specimens by 31.3% and 18.8% at 7- and 28-day tests, respectively.

These observations differ from previous findings regarding biochar-modified cementitious composites, where the inclusion of biochar enhances the early-age strength [10,19]. This difference may be associated with the larger pore size of hydrochar derived from HTC compared to biochar from pyrolysis, the potential presence of wooden organics in the hydrochar structure, and the differing pH levels of hydrochar and biochar. Yang et al. [20] indicated that shifting from pyrolysis to HTC could enlarge the size of pores and increase the pore volume of the byproducts from 2.24

nm to 7.82 nm and 0.006 cm^3/g to 0.067 cm^3/g, respectively. This increase may enhance the water-retention capacity of hydrochar; however, it could substantially reduce its strength and performance in cementitious composites. The study also showed that HTL decreases the values to 4.91 nm and 0.022 cm^3/g, respectively.

Prior results [20] also showed that the production technique could significantly affect the carbon content of the byproduct. The relationship between fixed carbon dosage and decomposition temperature indicates that biochar contains the highest fixed carbon, whereas hydrochar derived from HTC exhibits the lowest fixed carbon content. This might highlight the capability of hydrochar from HTC to release functional groups into the cement paste. The notable effect of the HTC-derived hydrochar on the 7-day CS of composites might also underscore the potential inclusion of wooden organics within the hydrochar structure. These organics could hinder the hydration reactions and increase the porosity of the cement paste. Earlier studies [20,21] suggested that raising the temperature of hydrolysis is an efficient technique to boost the fixed carbon percentage and possibly reduce the wooden organics in the hydrochar. This can be accomplished by switching from HTC to HTL.

Yang et al. [20] indicated that the byproduct of pyrolysis is an alkaline solid, whereas the byproducts of HTC and HTL are acidic solids. This pH alteration could considerably influence the performance of the hydrochar from HTC and HTL, as their dissolution could release acid into the cement paste, reducing its pH, impeding pozzolanic reactions, and potentially leading to the dissolution of surrounding hydration products.

Analyzing earlier data [17,18] also emphasized the vital role of biomass sources on the chemical composition of the hydrochar, affecting its reactivity, deterioration, and pH. As these factors could directly affect the performance of the hydrochar-modified composites [17], selecting a suitable biomass source for hydrothermal liquefaction could be a key factor in enhancing the effect of hydrochar in the composites. Moreover, investigating the effect of hydrochar from other biomass sources would provide a clearer picture of its potential as an SCM. Coffee wood is a potential biomass source that could improve the performance of the cementitious composite by up to 30% [22]. Therefore, it stands to reason that the hydrochar derived from spent coffee grounds could positively influence the properties of the composites. Besides, since the optimum biochar dosage was less than 1% concerning the OPC weight in several studies [23], it is crucial to ascertain the impact of lower substitution dosages than those used in Santos et al. [17](<1.25%).

Lastly, an earlier review demonstrated that biochar is more effective as an additive than as an SCM for enhancing mechanical strength [24]. This is because biochar is an inert material that accelerates the hydration reactions by providing retained water and nucleation sites [19]. As a result, replacing the reactive binders with biochar decreased the source of strengthening reactions, ultimately lowering the long-term strength of the biochar-modified cementitious composites [19]. A similar theory can be applied to hydrochar since the Chapelle index of the hydrochar at Santos et. al. [17] was limited to 43%, which may be lowered by increasing the hydrolysis temperature, reducing the pozzolanic potential of hydrochar [25]. Consequently, the effect of hydrochar as an additive on the mechanical properties of the cementitious mortars should be examined.

This study investigates the effect of incorporating hydrochar derived from HTL as a cement substitute and an additive on the mechanical strength, porosity, microstructure, and carbon footprint of cementitious mortars for the first time. Unlike the hydrochar from HTC, the effect of hydrochar from HTL on the mechanical properties of cementitious composites has not been investigated. However, given its physicochemical properties, it could be anticipated that the hydrochar from HTL could show a better performance in the composites than that of HTC. Given this potential, this research examines the effects of using 0%, 0.5%, 1%, and 2.5% hydrochar, produced from HTL of spent coffee grounds at 270°C and 20 bars for 20 minutes, as a cement alternative and an additive on the unit weight (UW), ultrasonic pulse velocity (UPV), compressive strength (CS), and microstructure of cementitious mortars at 7, 28, and 90 days. In this study, 63 cubic specimens in 7 mix designs were made and tested. The collected data assessed the impact of hydrochar derived from spent coffee grounds on the properties of mortars. The influence of hydrochar on the microstructure of mortars was analyzed through scanning electron microscopy and energy-dispersive X-ray spectroscopy. The effects of hydrochar derived from HTL and HTC on the mechanical properties of composites at different ages were also examined. The embedded carbon in hydrochar-modified cementitious composites was evaluated to assess the potential environmental advantages of incorporating hydrochar into cementitious mortars. By comparing the performance of HTL-derived hydrochar with that of HTC-derived hydrochar and biochar, this study offers new insights into the viability of hydrochar from HTL as an alternative SCM and additive, highlighting its potential for both improving the mechanical properties and reducing the carbon footprint of cementitious composites.

2. Methodology

2.1. Materials

In this study, blended cement with a specific surface area of 1608 m^2/kg (with the commercial name Lafarge GUb-25S/5SF) was used as the principal binder. The blended cement comprised 70% ordinary Portland cement, 25% ground granulated blast furnace slag, and 5% silica fume. Hydrochar with a specific surface area and volatile matter of 202.7 m^2/kg and 48.77%, respectively, (from the faculty of agriculture at Dalhousie University) was employed as either a supplementary cementitious material (SCM) or an additive. Hydrochar was a by-product of the hydrothermal liquefaction process. The spent coffee grounds from Tim Hortons were first dried at 105°C for 24 hours. The dried spent coffee grounds and distilled water were then mixed and placed in the sealed reactor (Parr 4590). Next, the nitrogen gas was purged into the reactor to remove air and pressurize to 20 bars. The reactor was then heated to 270°C. After 20 minutes of working at the temperature and pressure, the reactor was cooled, and the products were released. The hydrochar was then separated by filtration and dried at 105°C for 12 hours. Encouraged researchers could find detailed information about the hydrochar properties and production process in Yang et al. [20]. Masonry sand (from The Shaw Group Limited) with a water absorption of 1.22% in the saturated-surface-dry condition and tap water was also utilized for manufacturing mortar specimens. Table 1 displays the chemical characteristics of the materials measured using ELTRA CS2000 and inductively coupled plasma-optical emission spectrometry, respectively. Figure 1 illustrates the size distributions of the mix components. The particle size distributions of the binders, i.e., blended cement and hydrochar, and masonry sand were measured using the dry laser diffraction method and standard sieve analysis technique, respectively.

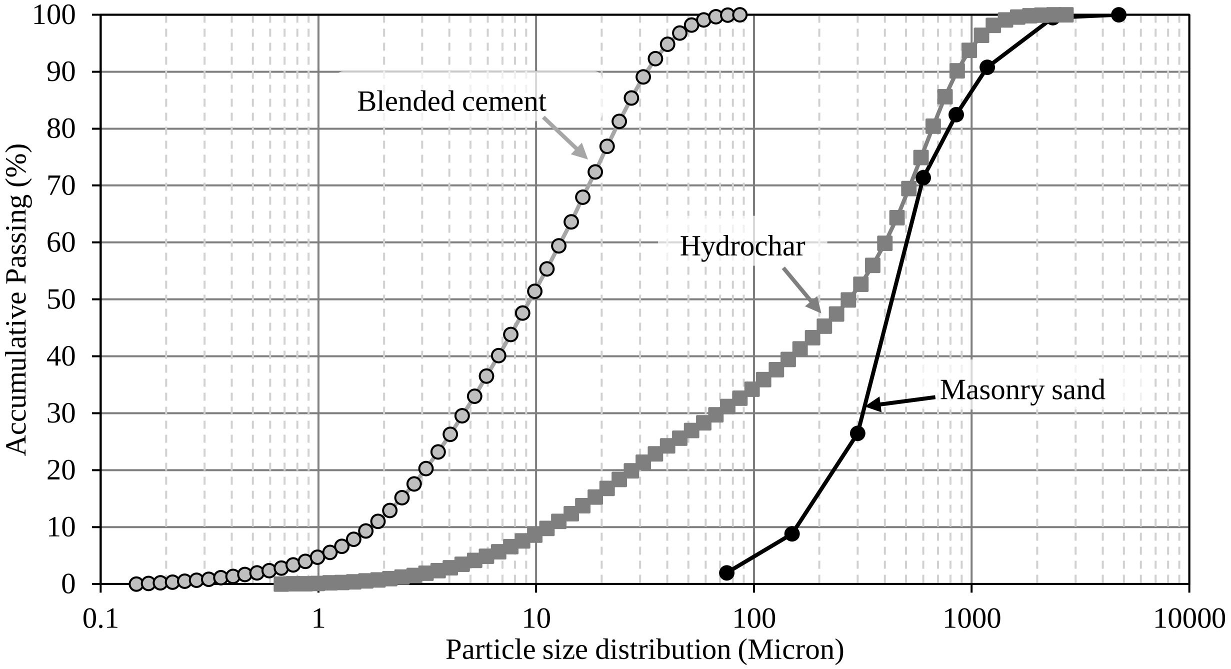

Figure 1. Particle size distributions of mix components

Table 1. Chemical compositions of the binders

Chemical element (%)	Ca	Si	Al	Fe	K	Mg	Na	S	C	H	N	Ash
Blended cement	38.42	12.85	3.03	1.33	0.84	1.51	0.09	1.11	-	-	-	-
Hydrochar	0.18	0.41	0.01	0.03	0.08	0.10	2.88	2.87	57.19	7.50	3.23	1.72

2.2. Test Matrix

Table 2 presents the reference mixture proposed by ASTM C109/C109M-21 [26] for nine cubic mortar specimens, with a dimension of 50×50×50 mm. Table 3 displays the dosages of substitution and hydrochar in each mix analyzed to assess the impact of hydrochar as an additive and an SCM in cementitious composites.

Table 2. Reference mix design for nine mortar cubes

Mix components	SSD* Masonry sand	Blended cement	Water
Weight (kg)	2035	740	359

* Saturated-surface-dry

Table 3. Mix designs

Group	Mix ID	Cement substitution dosage by biochar (%)	Hydrochar/ Cement as an additive (%)	Number of samples
SCM	Reference	0	0	9
	SCM-H0.5	0.5	0	9
	SCM-H1	1	0	9
	SCM-H2.5	2.5	0	9
Additive	Add-H0.5	0	0.5	9
	Add-H1	0	1	9
	Add-H2.5	0	2.5	9
Total				63

2.3. Specimen Preparation

This study followed ASTM C109/109M-21 [26] for manufacturing and curing the specimens. Manufacturing began with weighing and preparing the required materials. Next, the hydrochar and saturated-surface-dry masonry sand were combined in the mixer. Then, the blended cement was added to the mixer and combined with the sand and hydrochar. The water was then gradually supplemented with the mix. After achieving a homogenous mix, the mortar was cast into the lubricated molds with a dimension of 50×50×50 mm and tamped in two layers and four rounds according to ASTM C109/C109M-21 [26]. The specimens were sealed in plastic bags for the first 24 hours to minimize moisture loss. Afterward, the molds were removed, and the specimens were placed in the standard moist curing room with a humidity level of +95% and a temperature of 25±2℃ until the testing date. Figure 2 depicts the specimen preparation process.

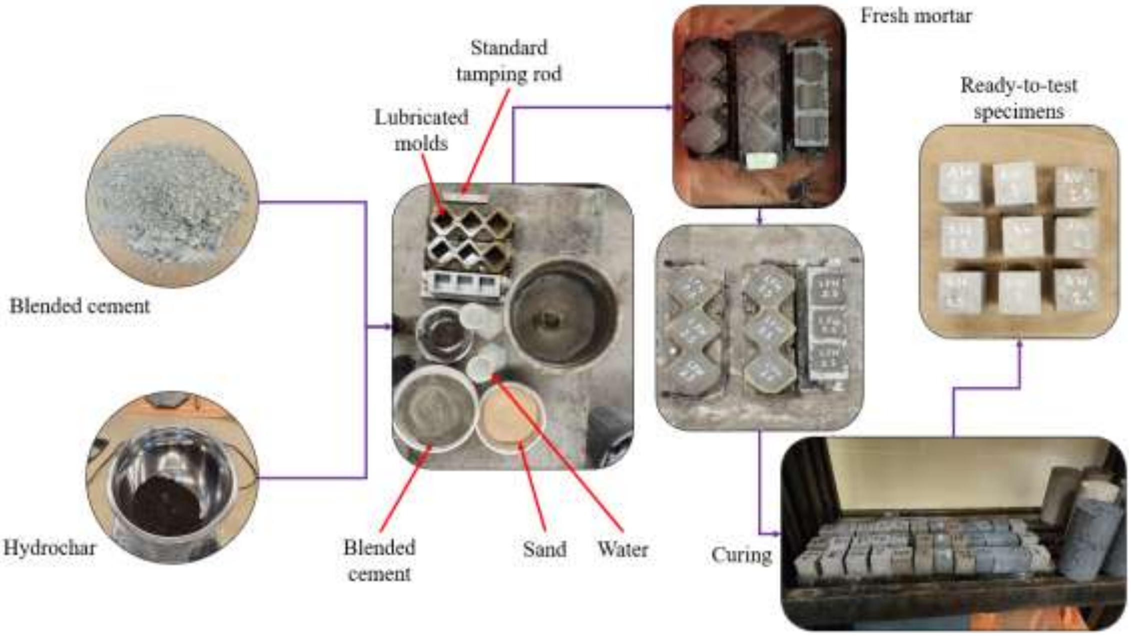

Figure 2. Specimen preparation

2.4. Testing

This study examined the variations in UW, UPV, CS, and microstructure of the mortar cubes at 7, 28, and 90 days. The specimens were taken from the curing room according to the testing dates and placed in normal air conditions at the lab for two days to ensure that the excess hydrochar-retained water was removed. This is because an earlier study [19] demonstrated that the water retained by the porous carbon-rich particles, biochar, could artificially raise the strength of cementitious composites, which could skew the results. The following tests were then conducted in a sequential order.

2.4.1. Unit Weight (UW)

In this study, the bulk density of the specimens was determined before UPV tests. First, the dimensions of the specimens were precisely measured by a digital caliper. The average of four measurements for each direction (two from each opposite side) of the specimens was considered its dimension. The averages were then used to calculate the volume of the specimens. The weights of the specimens were measured using a scale with an accuracy of ±0.01 gram. Next, the UWs of the specimens were calculated by dividing their weight by volume. The average UW of three specimens with a specific mix design at each testing date was employed for analysis.

2.4.2. Ultrasonic Pulse Velocity (UPV)

UPV is a popular non-destructive technique for assessing the porosity of cementitious composites. In this study, the test was conducted by transmitting ultrasonic pulses through the length of the specimens using two 50 kHz electro-acoustical transducers contacted on the opposite sides of the specimens. To improve the wave transition and contact between the transducers and the specimen's sides, a thin layer of liquid honey was used as a couplant.

First, the UPV equipment was set up using its calibration rod, lubricated by a thin layer of liquid honey. Then, the opposite sides of the specimens were coated by a thin layer of liquid honey, and the transducers were contacted to the sides. A consistent pressure was applied to the transducers to ensure full contact between them and the specimen. The displayed value was then recorded as the wave's travel time. The UPV of the specimen was computed by dividing the wave traveling length, measured by the caliper, by the traveling time. This study used an average of six measurements (two per specimen) to determine the UPV of the mix at a specific testing date.

2.4.3. Compression Test

The compression test was performed using a compression machine with a loading rate of 0.5 kip/sec in accordance with ASTM C109/109M-21 [26]. The average CS of three specimens was reported for each mix at a specific age.

2.4.4. Scan Electron Microscopy and Energy Dispersive X-ray Spectroscopy (SEM-EDS)

In this study, the effects of hydrochar on the microstructure of the specimens were analyzed using SEM-EDS. First, the tested specimens from the compression machine were dried in an oven at 110±5℃ for 24 hours to halt the cementitious reactions. The core of the specimens was then collected and sealed inside plastic Ziplock bags. Next, the Leica EM ACE200 instrument was used to diffuse a 20-nm layer of gold-palladium powder on top of the collected samples. The Axia ChemiSEM LoVac 1247447 scanning electron microscope was employed to capture the SEM images and collect EDS results.

This study utilized EDS to detect the chemical elements present in the cement paste. The results facilitated the precise detection of hydrochar particles in the paste, as these particles exhibited a high carbon (C) content compared to other components. The SEM-EDS results were then collected from the specified area and used for analysis.

3. Results and Discussions

3.1. Unit Weight (UW)

Figure 3 illustrates that incorporating hydrochar into the mortar, either as an SCM or an additive, resulted in a reduction in the unit weight (UW) of the specimens. In the SCM-Hx series, increasing the replacement level to 2.5% gradually reduced the UW by 6.1%, 4.25%, and 4% at 7, 28, and 90 days, respectively. Similarly, in the Add-Hx series, increasing the hydrochar content to 2.5% led to UW reductions of 6.24%, 4.76%, and 4.42% at the corresponding ages.

Two factors might account for these patterns. First, the lower density of hydrochar particles relative to other mortar constituents might contribute to the decreasing trend in the UW as the hydrochar dosage increases. Second, accelerated reactions in the cement paste surrounding hydrochar particles might create discrepancies in hydration rates. These inconsistencies might lead to temperature and shrinkage differences, resulting in the formation of microcracks within the cement paste.

The findings also indicate that the 28-to-7-day UW ratios of the SCM-Hx and Add-Hx series increased from 1.011 to 1.031 and from 1.011 to 1.027, respectively, as the hydrochar dosage rose from 0% to 2.5%. This increase may be attributed to the release of hydrochar-retained water and its role in enhancing hydration reactions. In this hypothesis, hydrochar provides additional water and chemical elements, particularly carbon, which may dissolve and contribute to the reformation of hydration products within the hydrochar's effective zone. These processes could enhance hydration, densify the hydration products surrounding the hydrochar, and partially fill microcracks. Such microstructural improvements may explain the increase in the 28-to-7-day UW ratio.

Due to the high water retention capacity of hydrochar, an excessive dosage may limit the availability of water needed for early-age reactions. However, over time, the released retained water and moist curing could enhance hydration reactions and mitigate this limitation. Additionally, the hydration products from delayed reactions could partially fill the hydrochar pores, reducing the system's porosity. These improvements may ultimately increase the water uptake (UW) of specimens containing hydrochar.

The findings further reveal that the 90-to-28-day UW ratios remained nearly constant, with variations of less than 0.3% in both series. This stability may result from a balance between the beneficial effects of hydrochar's pozzolanic and filling properties and the potential deterioration of hydrochar over time. Moreover, the acidity of hydrochar may influence the system's alkalinity, potentially reducing pozzolanic reactions and dissolving some hydration products near hydrochar particles. [27].

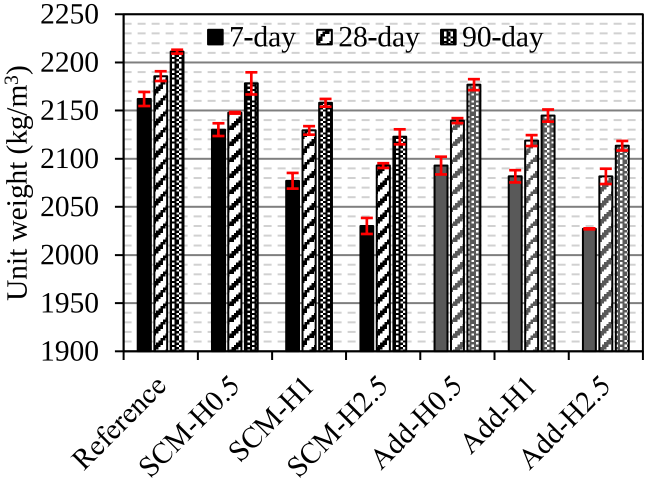

Figure 3. Average UW of the specimens at various ages

Figure 4 presents the variations in unit weight of specimens at 7, 28, and 90-day tests. The data indicated that while the effect of increasing hydrochar percentage on the UW of specimens was comparable in both series, using hydrochar as an additive had a slightly greater impact on the UW of specimens over time. The chart also exhibits that the UW reduction rate was slightly decreased by increasing the hydrochar dosage by over 1% in both series. This emphasizes the necessity of further studies to determine the factors influencing the decrease in the reduction rate. However, it could be suggested that potential causes may include the particle size distributions of the composite ingredients and the lower alkalinity of the system, which may contribute to reduced hydrochar deterioration.

Equation 1 represents the formulas applicable for predicting the 90-day UW of the specimens as the hydrochar dosage varies from 0 to 2.5% relative to the weight of binders. The proposed models could predict the UW of the SCM-Hx and Add-Hx series by the correlation coefficient (R^2) of 0.9982 and 0.9986, respectively. It is worth noting that these functions can be effectively applied to the same materials; however, their application to similar materials with different physicochemical properties may be beneficial for estimations in future studies.

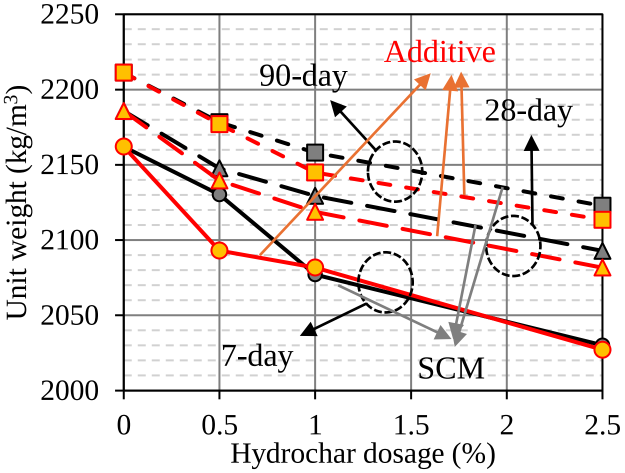

Figure 4. Effect of hydrochar dosage on the average UW of the specimens

$$UW(x) = \begin{cases} 12.471x^2 - 66.152x + 2210.3 & SCM - Hx \\ -17.54x^2 - 83.31x + 2212 & Add - Hx \end{cases} \quad for\ 0 \leq x \leq 2.5 \tag{1}$$

where UW and x are 90-day UW (in kg/m^3) and hydrochar percentage with respect to the weight of the binder (in %), respectively.

3.2. Compressive Strength (CS)

a) Hydrochar as an SCM

Figure 5 illustrates that the effect of substituting blended cement with hydrochar on the compressive strength (CS) of specimens was age-dependent. At 7 days, replacing 0.5% of the cement with hydrochar (SCM-H0.5) increased CS by 19.24%, whereas at 90 days, the same replacement resulted in a 16.01% reduction. These findings suggest that hydrochar derived from HTL, similar to biochar, significantly enhances early-age (7-day) hydration and strength in cementitious composites. This enhancement is potentially due to hydrochar’s ability to retain free water in the fresh mix, supply additional water for internal hydration, provide nucleation sites, refine pore sizes, and promote early carbonation. However, at higher dosages, hydrochar's porosity and the reduced reactive binder content in the system influenced CS negatively. Specifically, substituting 1% and 2.5% hydrochar led to 9.37% and 18.05% reductions in 7-day strength, respectively, compared to the reference specimens. This reduction may be attributed to increased water retention in hydrochar particles, which could limit the water available for initial hydration reactions. Even when the cement paste needed the retained water, capillary effects within the hydrochar pores might have hindered its release. Consequently, elevated hydrochar dosages probably reduced the availability of water for initial hydration, which had a notable effect on the 7-day CS. Nevertheless, moist curing appeared to alleviate these adverse effects at later times. The results are consistent with earlier studies [10,24] that suggested optimum biochar contents for early-age strength improvement in cementitious composites.

Figure 6 demonstrates that the optimum hydrochar percentage shifted from 0.5% at 7 days to 1% at 28 days. The data also indicated that specimens containing hydrochar exhibited increased strength of up to 9.57% compared to the reference specimens at 28 days. However, the pattern shifted to a descending trend at 90 days. This suggests that the hydrochar's influence on the mechanical properties of mortar reached its peak within the initial 28 days. It also pointed out the importance of 90-day strength for assessing the impact of hydrochar on the properties of cementitious composites.

The shift from optimal trends at 7 and 28 days to a descending pattern at 90 days might be ascribed to the reduced reactive cement content, the effects of hydration acceleration on the cement paste microstructure, hydrochar's pore structure, its lower reactivity compared to blended cement, its acidity, and its potential for deterioration. and disintegration. Reduced reactive cement limits the source of strengthening reactions, and when combined with hydrochar's lower reactivity, this could lead to a strength reduction in the long term.

Earlier studies [28] showed that rapid curing can negatively affect the long-term mechanical properties and microstructure of composites. Accelerated hydration could reduce the homogeneity of cement paste by enlarging pores, increasing shrinkage rates, and causing microcracks due to uneven hydration rates at different spots. Additionally, rapid hydration might decelerate subsequent reactions by forming a dense layer of hydration products on the cement particles, restricting the access of their unreacted parts to water. Given the increased early-age strength of hydrochar-modified specimens, it is reasonable to infer that similar hydration acceleration effects could contribute to the strength decline observed at 90 days.

Hydrochar's acidity (pH = 3.89) might also weaken the composite by lowering the system's overall pH, potentially reducing pozzolanic activity. Furthermore, hydrochar dissolution in the cement paste could release acidic compounds, which might dissolve surrounding hydration products and weaken the bond between hydrochar and cement paste [10]. Additionally, hydrochar's pore structure could increase system porosity, further contributing to strength reduction. Like biochar [29], hydrochar's low strength may lead to simultaneous failure of the hydrochar itself and its interfacial transition zone (ITZ) with cement paste under initial loads, facilitating crack propagation and reducing required crack length by creating weak spots.

Observations also revealed that some hydrochar particles were disintegrated within the specimens (refer to Figure 7). Figure 8 illustrates that the disintegration resulted in an expansion of the hydrochar particles, exerting internal pressure to the surrounding cement paste and causing microcracks. This also suggests that the particles might contain residual wooden organics, which could expand during curing and shrink upon moisture loss, thereby increasing the porosity of the specimens. These factors could weaken the interlock between the cement paste and hydrochar particles, creating weak spots in the specimens and facilitating crack propagation.

Considering the physicochemical properties of hydrochar and its similarities to biochar, exposure to cement paste may deteriorate hydrochar particles over time. The deterioration could coarsen the size of hydrochar pores, thin hydrochar’s shell, and release fulvic acid [13]. These factors could reduce the long-term CS of specimens by weakening hydrochar particles and their bond with cement paste.

Findings also displayed that the 28-to-7-day CS ratio was reduced by 17.14% at a 0.5% substitution dosage. Nonetheless, increasing the dosage to 1 and 2.5% enhanced the ratio by 20.9% and 27.32%, respectively, compared to the reference samples. The notable strength increase was potentially caused by the completion of initial reactions at later ages, as the lower 7-day strengths were likely due to the high water retention within hydrochar particles. The considerable reduction in the 28-to-7-day CS ratio at 0.5% replacement and the shift in optimal dosage between 7 and 28 days might also be explained by the effect of hydration acceleration on the microstructure of cement paste and the availability of unreacted cementitious components.

The data indicated that increasing cement replacement from 0% to 1% progressively decreased the 90-to-28-day strength ratio from 1.58 to 1.17. This suggests that hydrochar's effect on improving the strengthening reactions was limited to the first 28 days. This pattern could be attributed to reduced cement content, accelerated early-age hydration, as well as hydrochar particles' disintegration and deterioration. The reduction in cement content and early hydration acceleration limited the availability of reactive components for later reactions. The rapid cement paste curing might also induce microcracks and slow subsequent hydration. Hydrochar deterioration and particle disintegration over time could further weaken the material, continuously reducing particles' strength and interlocking with cement paste.

b) Hydrochar as an Additive

Figure 5 illustrates that incorporating hydrochar as an additive at dosages of 0.5% and 1% can enhance the 7-day CS of specimens by 59.59% and 56.07%, respectively. The strength advantages persisted at 28 days, when the addition enhanced the CS of specimens by 36.73 and 44.02%, respectively. Increasing the dosage to 2.5% resulted in a reduction of the CS advantage to 29.76% and 11.29% at 7 and 28 days, respectively, in comparison to the Reference series. The results highlighted the substantial impact of hydrochar as an additive in improving early-age strength by offering extra water, nucleation sites, and potentially dissolved carbon, as well as refining the size of pores and enhancing pozzolanic reaction. This acceleration could benefit the construction sector by reducing the required curing time for concrete strength development. The reduced 7- and 28-day strengths observed in specimens with 2.5% hydrochar, in comparison to those with 0.5% and 1%, can be attributed to three factors: 1) the dilution effect, 2) excessive water retention, and 3) the overfilling effect of hydrochar particles at elevated dosages, which leads to an increase in the number of voids within the system.

The 28-to-7- and 90-to-28-day CS ratios suggested that the acceleration of strengthening during the first 7 days led to a reduced strength gain in the subsequent 7-to-28- and 28-to-90-day periods. Consequently, the CS of reference specimens was across those containing hydrochar such that the specimens containing 0.5%, 1%, and 2.5% hydrochar had 0.01%, 5.77%, and 14.18% less strength than the reference specimens at 90 days, respectively. The porosity, disintegration, acidity, potential shrinkage, and deterioration of hydrochar particles, along with the adverse effect of hydration acceleration on the microstructure of cement paste in the long term, might contribute to the strength reduction by creating weak spots and microcracks in the composite, which promote crack propagation.

The 28-to-7- and 90-to-28-day CS ratios indicate that the rapid strengthening observed in the initial 7 days resulted in decreased strength gains during the following intervals. As a result, the reference specimens achieved higher strength than those containing hydrochar at 90 days. Consequently, the specimens with 0.5%, 1%, and 2.5% hydrochar exhibited 0.01%, 5.77%, and 14.18% lower CS compared to the reference specimens at 90 days, respectively. The porosity, disintegration, acidity, potential shrinkage, and deterioration of hydrochar particles, combined with the negative impact of hydration acceleration on the microstructure of cement paste, may lead to strength reduction by forming weak spots and microcracks in the composite and thereby facilitating crack propagation.

The comparison of hydrochar's effects as an SCM and an additive indicated that the latter resulted in a superior strength at all ages. Incorporating 0.5% hydrochar as an additive enhanced the CS of specimens by 59.59% and 36.73% at 7 and 28 days, respectively. However, replacing cement with an equivalent percentage of hydrochar in the SCM-Hx series resulted in a 19.24% increase in compressive strength (CS) at 7 days, while causing a 1% decrease in strength at 28 days. Adding hydrochar as an additive also demonstrated a minimal effect on the 90-day CS of the specimens. The cement content and properties of hydrochar may account for this disparity in its effect as an SCM versus an additive. Increasing the percentage of hydrochar in the SCM-Hx series corresponded with a decrease in cement content. This factor, along with the lower reactivity of the hydrochar, could reduce the quantity of strengthening reactions in the specimens, referred to as the dilution effect, which potentially undermines the composite's strength over time. However, adding hydrochar as an additive did not affect the cement content, thereby having no adverse impact on the quantity of strengthening reactions. Adding hydrochar as an additive could also raise the CS of specimens by promoting early carbonization, refining the size and number of voids in cement paste, and providing pozzolans. Interaction among these factors might lead to a notable strength improvement in the Add-Hx series relative to the SCM-Hx series across all ages.

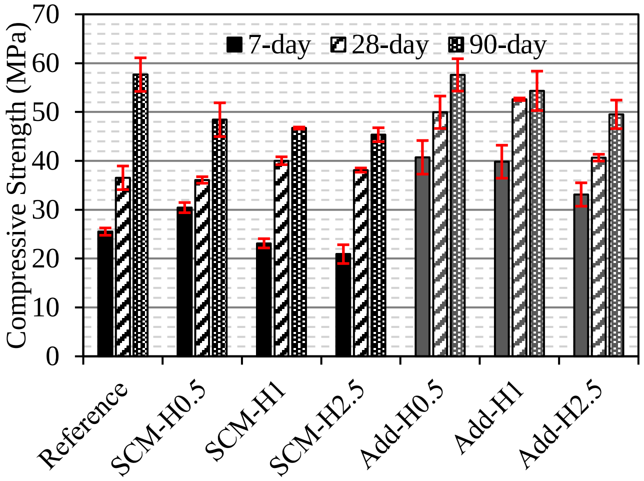

Figure 5. Average CS of the specimens at various ages

Figure 6 displays the disparity in CS for the SCM-Hx and Add-Hx series. The data indicated that the notable difference in the effects of hydrochar in the Add-Hx and SCM-Hx series at 7 days converged more closely at 90 days. The results also showed that the trend gradient in the Add-Hx series increased following a 0.5% dosage, whereas the slope in the SCM-Hx series decreased after the 0.5% dosage at the 90-day measurements. Equation 2 presents the models applicable to estimate the 90-day CS of the SCM-Hx and Add-Hx series, with the correlation coefficients (R^2) of 0.9487 and 0.9608, respectively.

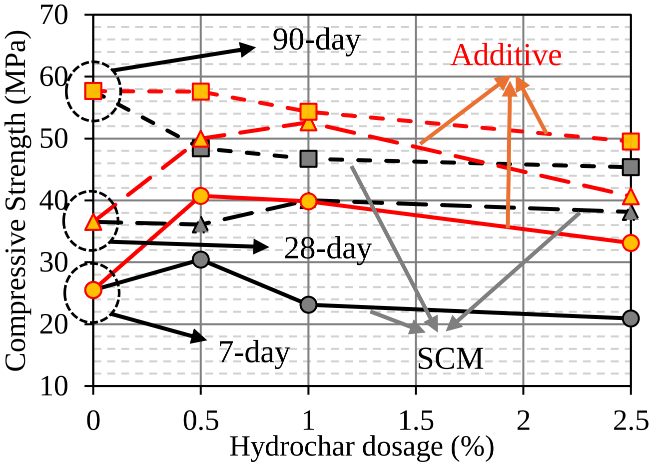

Figure 6. Effect of hydrochar dosage on the average compressive strength of the specimens

$$CS(x) = \begin{cases} 4.892x^2 - 17.101x + 57.66 & SCM - Hx \\ -3.1614x + 57.66 & Add - Hx \end{cases} \quad for\ 0 \leq x \leq 2.5 \tag{2}$$

where CS and x are the CS of specimens (in MPa) and hydrochar dosage concerning the weight of the binder (in percent), respectively.

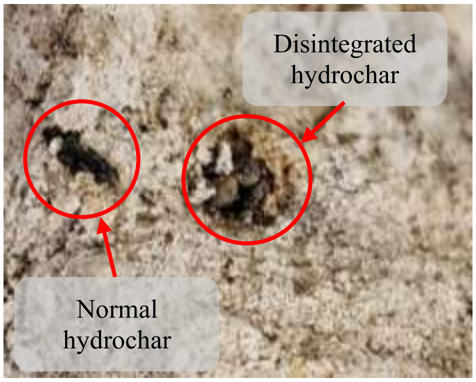

Figure 7. Disintegrated hydrochar particle in specimens

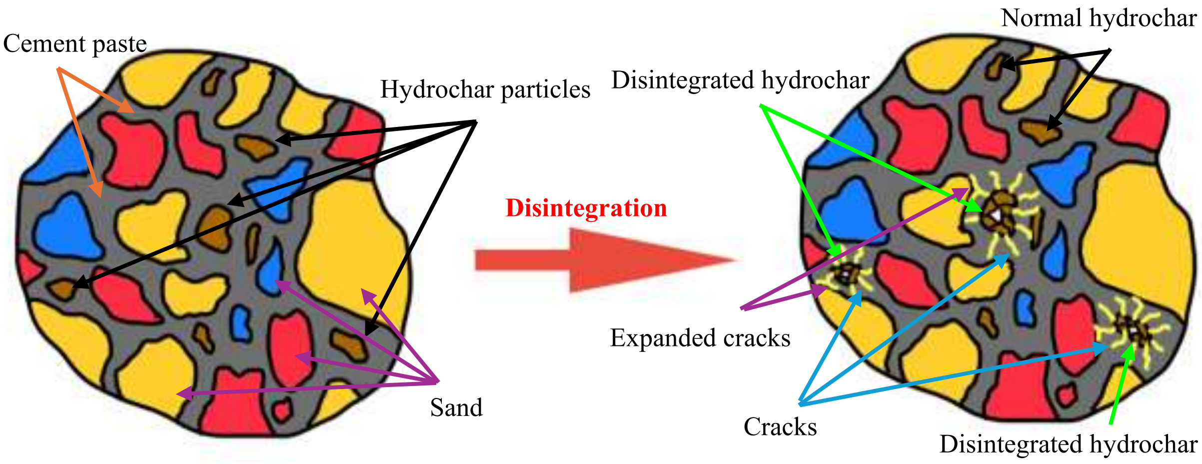

Figure 8. Hydrochar disintegration

3.3. Ultrasonic Pulse Velocity (UPV)

Figures 9 and 10 depict that increasing hydrochar dosage to 2.5% consistently reduced the UPV of the specimens in all ages. Since the UPV can estimate the porosity of the specimens, the data indicated that the incorporation of hydrochar as either an SCM or an additive raised the specimens' porosity. This is consistent with the unit weight results shown in Figure 3. The reduction in UPV can be attributed to the low density and high porosity of hydrochar particles as well as its effect on promoting microcracks in the surrounding cement paste. The results also showed that the specimens' 28-to-7-day and 90-to-28-day UPV exhibited minimal effect (less than 2%) when hydrochar dosage ranged from 0 to 2.5%.

Comparing the enhancement rates for UPV and UW over time indicated that UPV enhancement rates exceeded those of UW from 7 to 90 days. The principles of strengthening reactions and wave transmission may elucidate these discrepancies. In the strengthening reactions of cementitious composites, water interacts with binders to produce a solid microstructure. In accordance with the mass conservation law, the weight of the system remained nearly constant during the reactions. However, the formation of the solid part increased the UPV since the wave transmits faster in solid materials than in liquids.

Findings also showed that increasing the hydrochar dosage to 2.5% decreased the disparity between the enhancement rate of UPV and UW. This might be attributed to the acceleration in the initial strengthening reactions as well as the impact of replacing retained water with air in the hydrochar pores, which lowers the UPV improvement of specimens with hydrochar over time.

The data also indicated that replacing 0.5% of cement with hydrochar reduced the UPV of the specimens by 1.31%, 0.82%, and 1.19% at 7, 28, and 90 days, respectively. The results also indicated that substituting 1% of cement with hydrochar led to a 2.26% reduction in the 28-day UPV of the samples. These findings contrasted with the CS observations, where 0.5% and 1% substitutions increased strengths at 7 and 28 days, respectively.

Figure 9 exhibits that while using hydrochar as an additive significantly enhanced the 7- and 28-day strengths of the specimens, it concurrently decreased their UPV at all ages. For example, incorporating 2.5% hydrochar reduced the 7-, 28-, and 90-day UPV by 5.66%, 6.14%, and 4.14%, respectively. This suggests that although increasing the hydrochar content raised the porosity of the composite, it simultaneously boosted the CS of specimens in the Add-Hx series.

The unique strengthening mechanisms of hydrochar that enhance hydration reactions could account for this variation. Typically, SCMs and additives comprise dense or reactive solid powders that boost strength via filler or pozzolanic effects. Consequently, their incorporation decreased the porosity of the system. However, hydrochar is a carbon-rich porous material that promotes strengthening reactions by providing extra water, nucleation sites, and dissolved carbon. It could also refine the size and number of pores. This process improves the strength of the surrounding cement paste while also elevating the system's porosity. This is consistent with Zhu et al. [30], suggesting that the water supplied by biochar improved the ITZ of cement paste surrounding the biochar pores and increased its porosity.

Despite the higher strength of the Add-Hx series, the data showed that the SCM-Hx set had higher UPV and lower porosity, which is consistent with the UW results. The more reactive binder in the Add-Hx set likely boosted the strength of the specimens compared to the SCM-Hx series. However, replacing a portion of dense aggregates in the Add-Hx series with hydrochar may increase the specimens' porosity, resulting in a lower UPV relative to the SCM-Hx series. The data also showed that the Add-Hx series achieved a 1.3% lower UPV improvement relative to the SCM-Hx set over the 7-to-28-day period. However, the 90-to-28-day UPV ratio of the Add-Hx series was gained from 1.035 to 1.057 by increasing the hydrochar dosage from 0 to 2.5%.

Figure 10 shows the effect of varying hydrochar dosages on the UPV of specimens. Despite the distinguished differences in the 28-day data among the series, the UPV of the series nearly converged to a similar function at 90 days, with a minor variation of 1.1% in specimens with a 0.5% hydrochar dosage. The data also indicated that the influence of hydrochar dosage on the UPV of the composites could be modeled by a linear function, shown in Equation 3, with correlation coefficients of 98.92% and 84.34% for SCM-Hx and Add-Hx series, respectively.

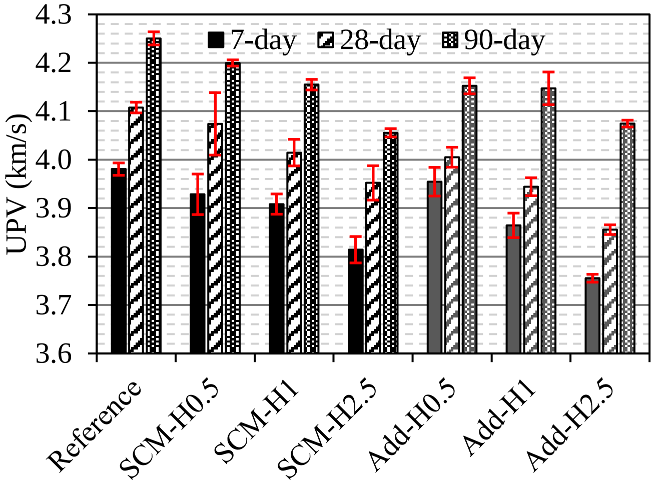

Figure 9. Average UPV of the specimens at various ages

$$UPV(x) = \begin{cases} -0.0814x + 4.251 & SCM - Hx \\ -0.0792x + 4.251 & Add - Hx \end{cases} \qquad 0 \leq x \leq 2.5 \tag{3}$$

where UPV and x are the ultrasonic pulse velocity (in km/s) and hydrochar percentage (in percent), respectively.

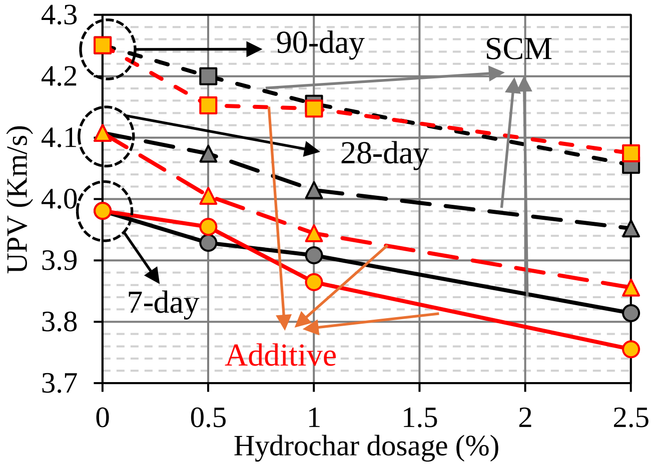

Figure 10. Effect of hydrochar dosage on the average UPV of the specimens

Figure 11 illustrates the relationship between the UPV and CS of the specimens. The findings indicated no clear correlation existed between UPV and CS at 7 and 28 days. However, the 90-day CS of the SCM-Hx and Add-Hx can be modeled by UPV with correlation coefficients (R^2) of

0.9683 and 0.9000, respectively (Equation 4). This could be attributed to the diminished effect of the interplay between hydrochar's ability to enhance strengthening reactions and reduce the available water for initial reactions.

$$CS(UPV) = \begin{cases} 604.96UPV^2 - 4964.8UPV + 10231 & SCM - Hx \\ 395.24UPV^2 + 3337.2UPV - 6986.3 & Add - Hx \end{cases} \quad \begin{matrix} 23 \leq CS \leq 58\ \& \\ 3.69 \leq UPV \leq 4.26 \end{matrix} \tag{4}$$

where CS and UPV are the compressive strength (in MPa) and UPV (in km/s) of mortar specimens, respectively.

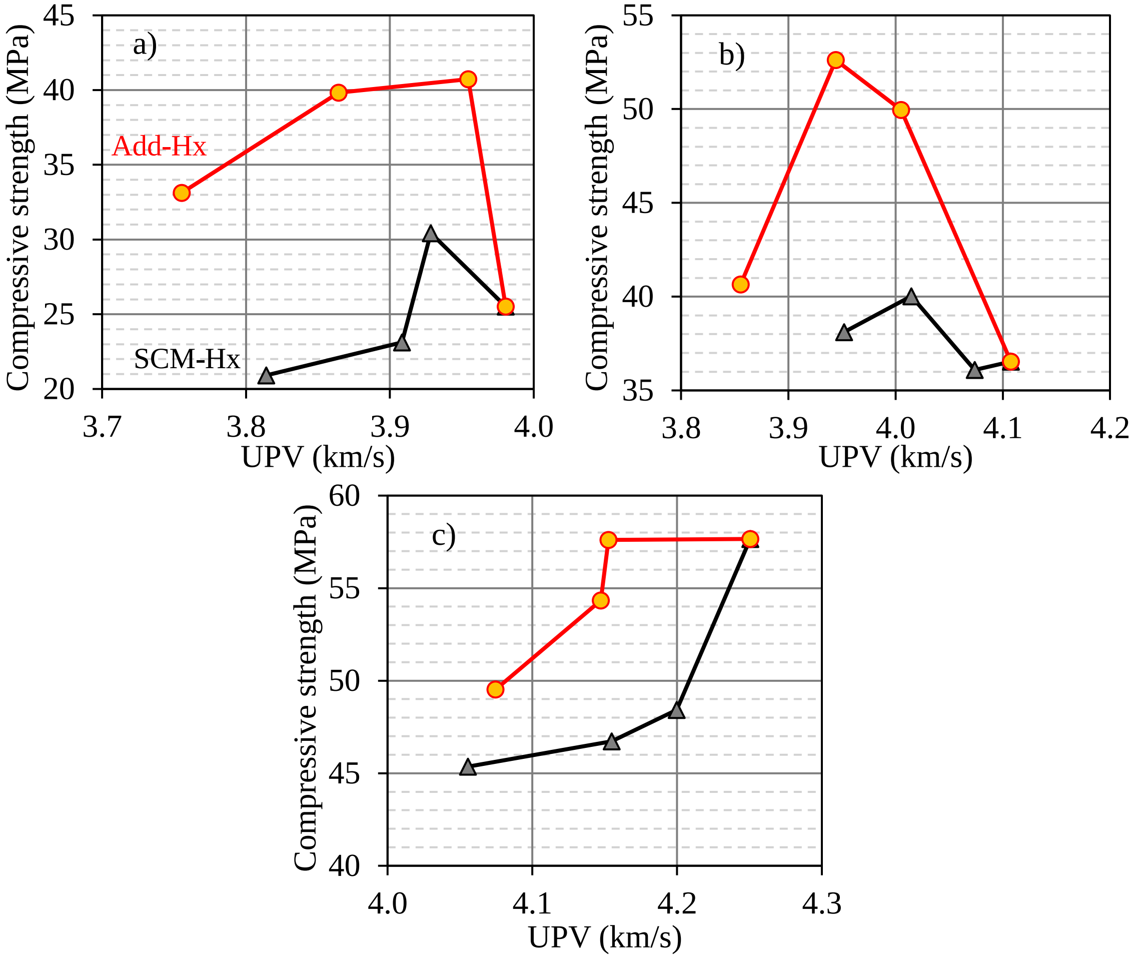

Figure 11. Correlation between UPV and compressive strength of the specimens at a) 7 days, b) 28 days, and c) 90 days

3.4. Microstructural Analysis

3.4.1. Effect of Hydrochar on Cement Paste

Figure 12 shows the ITZ between aggregate-cement paste and cement paste-hydrochar in reference specimens and specimens with 2.5% hydrochar at 90 days. Table 4 presents the SEM-EDS findings regarding the effect of using hydrochar in cementitious mortars. The results showed that the hydration products formed in the aggregate-cement paste ITZ were denser than those formed in the hydrochar-cement paste. The images also displayed that the hydration products formed adjacent to the hydrochar particles were primarily calcium carbonate, emphasizing the interaction between hydrochar and surrounding cement paste. However, the hydration products formed in the aggregate-cement paste ITZ were mainly calcium hydroxide and ettringite. The analysis also underscores larger gaps and higher levels of discontinuities in the hydrochar-cement paste ITZ compared to the aggregate-cement paste.

The EDS data suggested that incorporating hydrochar into the system increased the carbon (C) content in the hydration products from 12.85% to 21.3% in the cement paste adjacent to the hydrochar. Nonetheless, the calcium (Ca) concentration in the products formed near the hydrochar markedly reduced from 24.33% and 31.00% in zones 1 and 2 to a range of 12% to 20% at points 3 and 5. This may show the potential of hydrochar to raise the carbonization of the cement paste. Despite this reduction, using hydrochar increased the concentrations of Si and Mg in the area by up to 88.00% and 330.77%, respectively. The findings also indicated that hydrochar's influence on the chemical constituents of hydration products was confined to its immediate surroundings. Distancing from the hydrochar mitigated its influence on the chemical composition of the cement paste. These factors may underscore hydrochar's potential local field effect and its capacity to alter the percentage of chemical elements according to their closeness to the hydrochar particle.

The findings also pointed out that after 90 days of exposure to the cement paste, the C content of the hydrochar shell decreased from 57.19% to 38.6%. This emphasized the chemical interaction between the cement paste and hydrochar, exhibiting the potential for disruption in the cross-linking network structure of COOC and C-O-C within hydrochar shells. The deterioration and disintegration may elucidate the variation in the quantities of Ca and C within the hydration products surrounding the hydrochar particles.

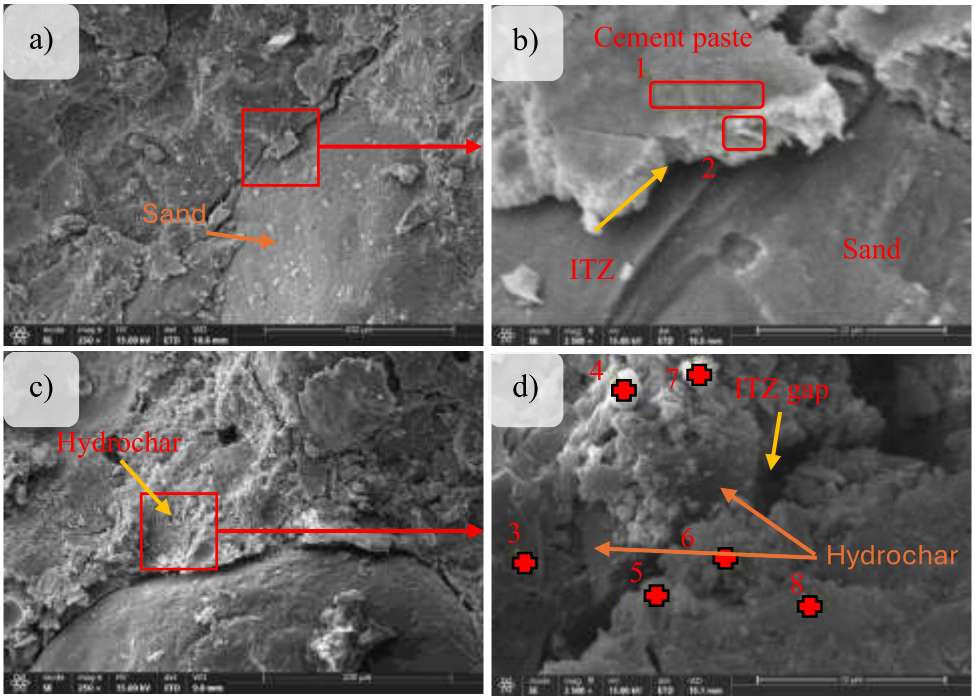

Figure 12. SEM of a & b) Reference and c & d) SCM-B2.5 specimens at 90 days

Table 4. EDS results of points and zones selected in Figure 12

Zone or point number	Chemical element (wt%)								
	C	O	Na	Mg	Al	Si	S	Ca	Fe
1	15.3	47.1	0.4	0.5	1.8	9.3	0.0	24.3	1.3
2	10.4	39.8	0.0	1.3	3.0	12.5	0.0	31.0	2.1
3	38.6	37.4	0.0	0.2	0.4	1.3	1.5	19.7	0.9
4	22.4	45.9	0.0	0.3	0.7	23.5	0.0	5.1	2.0
5	20.2	48.9	0.0	5.6	3.3	9.0	0.1	12.0	0.9
6	15.1	30.1	0.0	3.2	6.1	17.9	0.0	26.9	0.7
7	15.6	47.9	0.0	1.0	2.0	10.3	0.0	22.4	0.8
8	18.5	44.6	0.0	0.3	1.8	12.4	0.0	21.2	1.1

3.4.2. Hydrochar Disintegration, Deterioration, and Shrinkage

Figure 13 displays SEM images of the disintegrated hydrochar particle in the specimens containing 2.5% hydrochar at 90 days. The findings showed that the disintegration might induce internal pressure within the surrounding cement paste, leading to the formation of microcracks. It could also raise the system's porosity by enlarging the size of voids within the paste. These two factors could compromise the integrity of the cement paste by creating weak spots and facilitating crack propagation, leading to a reduction in the CS of specimens containing hydrochar.

Table 5 indicates a reduced carbon dosage within the disintegrated hydrochar compared to its side shells. The data also suggested that the internal portion of the hydrochar contained Si and Al at levels of 6.2% and 9.7%, respectively, which were higher than the values observed at points 1 and 2. The findings also showed that the internal portion of hydrochar had approximately 29% lower oxygen content. These chemical disparities between the internal and external regions of the hydrochar and the disintegration may raise concerns regarding the chemical stability of hydrochar within the composite. Furthermore, the decreased carbon and oxygen levels in the disintegrated particle may indicate a lower degree of hydrothermal decomposition in the particle's core relative to its shell. This may increase the likelihood of wooden organics and their negative effects on cementitious composites. Analyzing Figure 7 also indicated that larger hydrochar particles had a higher likelihood of disintegration compared to the smaller ones. This might emphasize the effect of particle size distribution on hydrochar particles' performance in cementitious composites.

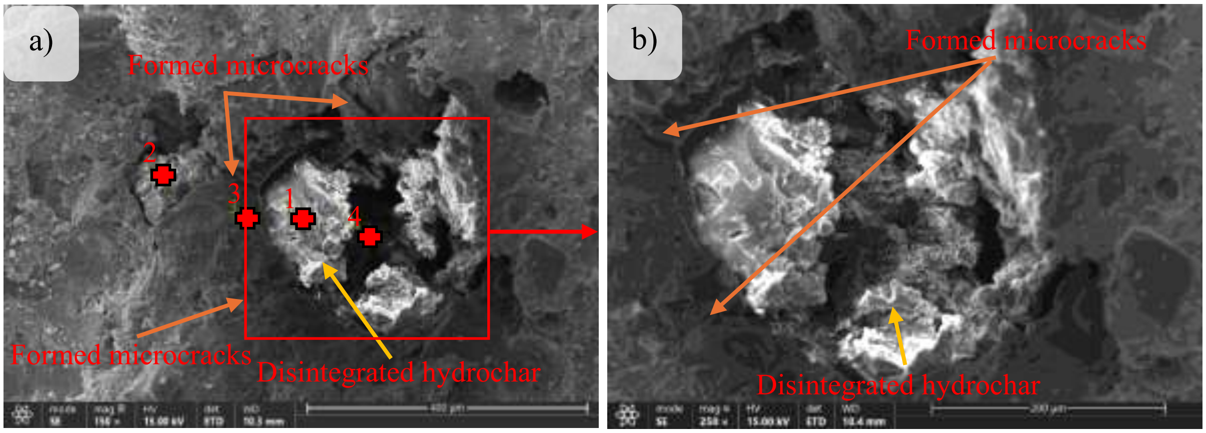

Figure 13. SEM of disintegrated hydrochar particles

Table 5. EDS results of points and zones selected in Figure 13

Area or point number	Chemical element (wt%)								
	C	O	Na	Mg	Al	Si	S	Ca	Fe
1	44.3	42.0	0.0	0.1	0.3	0.3	0.9	11.5	0.5
2	41.0	43.7	0.0	0.0	0.3	0.6	0.3	13.3	0.7
3	15.9	44.3	0.0	0.4	2.2	12.9	0.0	23.1	1.1
4	31.8	30.5	0.0	1.4	9.7	6.2	0.1	15.7	4.6

Figure 14 presents the SEM image of a deteriorated hydrochar particle within the specimens. SEM images revealed this as the most severe scenario, indicating the maximum potential deterioration of hydrochar in the specimens. In this case, a portion of the hydrochar particle dissolved, aiding its separation from the cement paste during sampling.

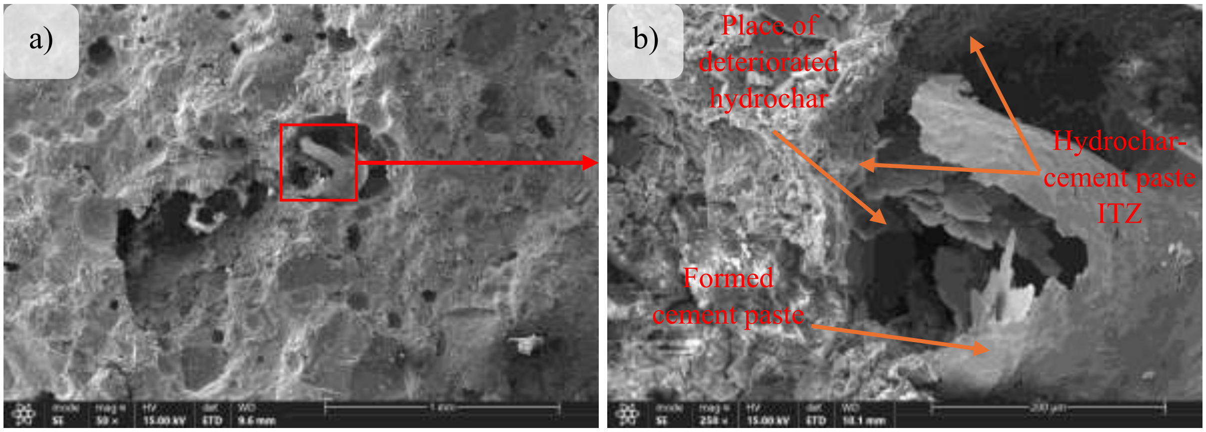

Figure 14. The deteriorated hydrochar in the mortar with a) 50x and b) 250x magnifications

The notable deterioration and disintegration of the hydrochar particles raised concerns regarding chemical stability and the wooden organics within the hydrochar. The change in the chemical stability of the particles could cause deterioration and disintegration. The wooden organics in the hydrochar might also impact the cement paste by their expansion during curing and shrinkage following the water removal. The topic particularly captured the authors' attention, as the hydrochar particles were effortlessly detached from the specimens during SEM sampling. The shrinkage may reduce the interlock within the cement paste-hydrochar ITZ, resulting in the formation of voids in the specimens. Figure 15 illustrates two hydrochar particles within the cement paste. Figure 15a displays a hydrochar particle entirely separated from the cement paste on all sides. This detachment highlights the potential shrinkage of the hydrochar particle. Conversely, Figure 15b demonstrates a hydrochar particle exhibiting good interlocking with cement paste. The particle size analysis indicated that larger hydrochar particles may possess a greater concentration of wooden components, potentially resulting in their shrinkage and detachment from the cement paste. Table 6 shows that the shrank particle had a lower carbon content (22.08%) in comparison to the values of 39% and 44% reported in Tables 8 and 9, respectively, while demonstrating higher dosages of aluminum, silicon, and calcium. This demonstrated the reduced carbonization of larger particles during hydrothermal liquefaction and the increased proportion of wooden organics.

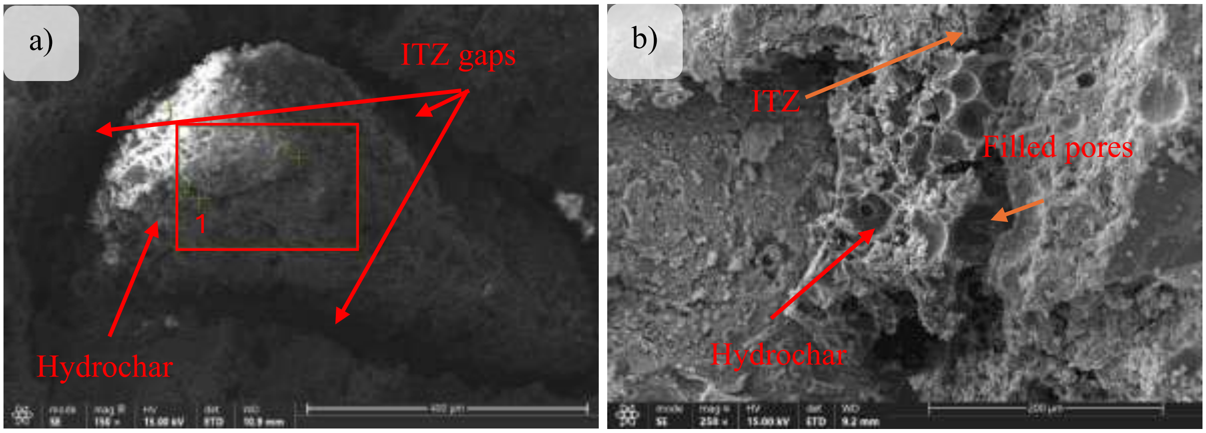

Figure 15. Different types of hydrochar particles in the specimens a) detached hydrochar and b) connected hydrochar to the cement paste

Table 6. The chemical composition of area 1 in Figure 15-a

Chemical element (wt%)								
C	O	Na	Mg	Al	Si	S	Ca	Fe
22.08	40.1	0.00	0.5	2.2	8.1	0.0	23.4	2.9

Consequently, due to the hydrochar's higher level of deterioration noted in this study compared to biochar [13], its disintegration, and its potential shrinkage, it can be concluded that hydrochar requires post-processing steps to enhance its chemical stability and carbonization prior to application in cementitious composites, thereby ensuring a uniform chemical composition throughout the hydrochar particles.

3.4.3. Hydrochar vs Biochar

This section provides a comparison between the physical properties of these particles with biochar derived from thermal decomposition of the same spent-coffee grounds at 500 °C via slow pyrolysis for 60 minutes. Figure 16 presents the SEM images of hydrochar particles. An earlier study [20] showed that shifting from pyrolysis to HTL could increase the average size of pores and total pore volume of particles from 2.24 nm to 4.91 nm and 0.006 cm^3/g to 0.022 cm^3/g, respectively. This increase might be caused by the effect of hot water as an organic solvent in the process [31]. Accordingly, the water dissolved more organics in the biomass, resulting in a higher porosity.

The increased porosity and larger pore sizes of hydrochar, when compared with biochar, may improve its water retention capacity. This might enhance the compactness and effect of hydrochar on the hydration acceleration of cementitious composites. Nonetheless, the higher porosity of hydrochar could reduce its load-bearing capacity. This could negatively impact the CS of the composites modified by hydrochar compared to those modified by biochar.

Analyzing the biochar used in earlier literature [10,19] also highlighted a significant difference between the structures of hydrochar and biochar. The findings displayed that hydrochar particles had a subangular morphology, while biochar particles were characterized by an angular and needle-like shape. Furthermore, the pores in biochar predominantly exhibited unidirectional orientation, whereas the pores in hydrochar lacked a specific directional alignment. Consequently, the arrangement of the pores constrained its beneficial impact on delivering supplementary water to both ends. In contrast, the hydrochar-retained water was released uniformly from all sides, enhancing the reactions surrounding the particles.

The physical shape analysis also revealed that while biochar angularity enhances interlock within the cement paste, hydrochar particles do not primarily contribute to strength improvement through interlock effects. The subangular shape of the hydrochar and its potential for shrinkage may weaken its ITZ with the cement paste, thereby facilitating crack initiation and propagation and decreasing the strength of the composite.

From a chemical perspective, examining the deterioration level of hydrochar and biochar particles [19] indicated that hydrochar's lower chemical stability than biochar. Furthermore, the absence of disintegration and shrinkage in biochar-modified cementitious composites

[13,19,30,32] suggested that the hydrochar might contain a higher concentration of wooden organics. From the technical perspective, this might be explained by the higher fixed carbon and carbonization in the biochar compared to hydrochar [20]. Increasing the dosage of fixed carbon could maximize the stability of the carbon-rich solid and lower its susceptibility to biological decomposition. Yang et al. [20] indicated that hydrochar contains more liable carbon and functional groups than biochar, which is primarily composed of recalcitrant carbon. The higher dosage of liable carbon in hydrochar could accelerate its deterioration and increase its interaction with water. These could speed up hydrochar's deterioration compared to biochar and raise significant concerns regarding the long-term properties of hydrochar-modified cementitious composites.

From a pH viewpoint, biochar is characterized as an alkaline solid with a pH range of 6.4 to 10.5 [33–35], while hydrochar is classified as an acidic solid with a pH of 3.89. The variation in pH can significantly affect the performance of materials in cement paste. The low pH of hydrochar can substantially lower the pH of cement paste close to the particles. Accordingly, its exposure to the cement paste could negatively charge its surface, which could be caused by deprotonation of the functional groups. This phenomenon could accelerate the hydrochar’s deterioration, result in the leaching of soluble organic components to the cement paste, hinder the cement hydration, and repel the calcium ions. However, the alkalinity of biochar may slightly affect the pH of the cement paste. In this mechanism, the alkalinity of biochar could attract the calcium ions given its negatively charged surface, promoting the formation of dense C-S-H gels. Based on these explanations, the low pH of hydrochar could raise concerns regarding the long-term properties of hydrochar-modified composites, particularly their acid and corrosion resistance. However, the alkalinity of biochar could alleviate concerns regarding the long-term durability and corrosion resistance of biochar-modified composites. Therefore, detailed studies are required to assess the durability properties of the hydrochar-modified concrete.

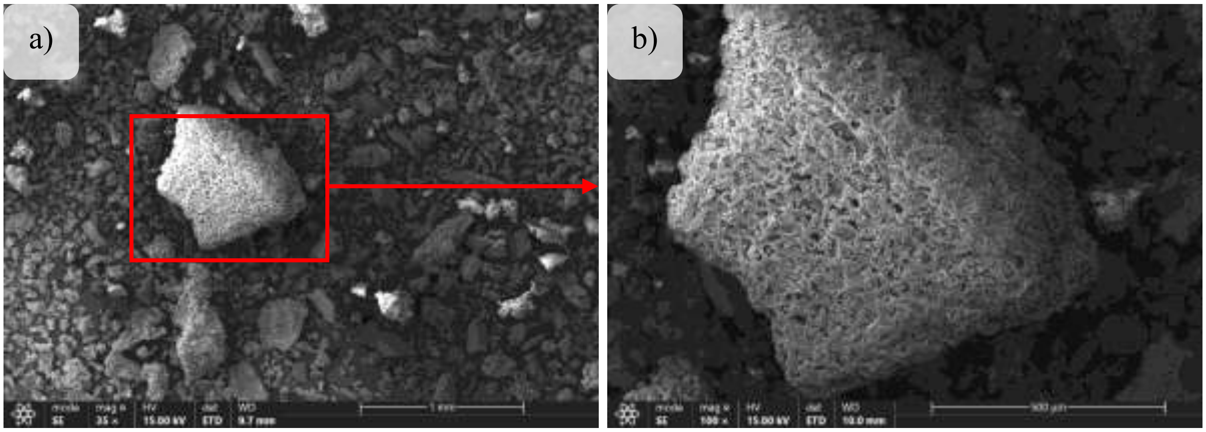

Figure 16. SEM image of hydrochar particles used in this study with a) 35x and b) 100x magnifications

4. Comparison with Earlier Studies

Santos et. al. [17] found that incorporating hydrochar derived from the hydrothermal carbonization of rice husk and stabilized organic fraction led to a significant reduction in the CS of the system at 7 and 28 days, achieving decreases of up to 60% and 26%, respectively, at a substitution rate of 1.25%. Their results also indicated a notable strength enhancement in specimens containing 1.25% hydrochar derived from rice husk between 28 and 90 days, which was attributed to the pozzolanic activity of the hydrochar particles. Similar findings were reported by Sharma et al. [18], who investigated hydrochar produced from the hydrothermal carbonization of pomegranate peel at 250°C for 4 hours as a supplementary cementitious material (SCM) in cementitious mortars. Their results showed that incorporating hydrochar at dosages ranging from 0 to 1% reduced the compressive strength of mortar specimens by 31.30% and 12.8% at 7 and 28 days, respectively.

The variation in hydrochar's effect on cementitious mortars may be attributed to the influence of hydrothermal decomposition conditions on its physicochemical properties. Hu et al. [21] demonstrated that increasing the temperature and residence time in hydrothermal carbonization from 150°C to 210°C and from 30 minutes to 120 minutes enhanced the degree of carbonization, leading to an increase in carbon content and a decrease in the O/C and H/C ratios. A higher carbon dosage suggests greater hydrochar stability. An earlier study [20] also indicated that increasing the hydrothermal temperature and duration reduced the presence of wooden organics in hydrochar, which may mitigate their adverse effects on hydration reactions and hydrochar degradation in cement paste. This hypothesis is consistent with the observation that specimens containing hydrochar produced at 250°C for 4 hours [18] showed a lesser reduction in strength compared to those with hydrochar derived at 200°C for 2 hours [17].

In contrast to the previous studies [17,18], the current investigation revealed that replacing blended cement with hydrochar obtained from the HTL of spent coffee grounds at substitution rates of up to 2.5% improved the compressive strength of mortars during the initial 28 days. Nonetheless, the high porosity and low reactivity of the hydrochar resulted in specimens with 1% hydrochar showing a 16% decrease in 90-day compressive strength compared to the reference samples.

The observed shift in hydrochar's effect on early-age strength may be attributed to differences in the physicochemical properties of hydrochar produced via HTL and HTC. Yang et al. [20] reported that transitioning from HTC to HTL increased the fixed carbon content from 33.14% to 49.21% and decreased the O/C ratio from 0.23 to 0.15, indicating a higher degree of aromaticity, greater stability, and a lower concentration of wooden organics in HTL-derived hydrochar. This difference may explain the improved early-age strength in the current study, as wooden organics in HTC-derived hydrochar may have hindered early hydration reactions in previous studies [17,18]. Additionally, the lower O/C ratio in HTL hydrochar could enhance its hydrophobicity, reducing excessive water absorption and thereby minimizing the negative impact of hydrochar on the availability of water for early hydration reactions.

Yang et al. [20] indicated that HTL processing led to a decrease in the total pore volume and average pore size of hydrochar obtained from spent coffee grounds, changing from 0.067 cm^3/g and 7.82 nm to 0.022 cm^3/g and 4.91 nm, respectively. Consequently, the HTL produced denser hydrochar than HTC, which might raise the strength of the hydrochar and improve its performance in the composites. Besides, HTC-derived hydrochar exhibited a significantly larger surface area (15.15 m^2/g) compared to that of HTL (7.74 m^2/g). This, together with the higher dosage of functional groups in HTC-derived hydrochar [20], might increase the chemical interaction between the hydrochar derived from HTC compared to that of HTL, raising its susceptibility to deterioration.

5. Embedded Carbon

In this study, embedded carbon was measured using the CO_2-equivalent (CO_2-eq) of the mix components in the material phase. Emissions from the transformation and storage phases were excluded, as they depend on variables such as transportation distance, vehicle type, and storage system.

Since this is the first study to assess the CO_2-eq of hydrochar, it followed the method proposed by Gupta and Kashani [36] to estimate the carbon sequestration of carbon-rich materials. This method assumes that, if not thermally decomposed, biomass would be burned for energy production, releasing its entire carbon content. Therefore, the carbon content of the hydrochar by-product can be considered sequestered.

The hydrochar used in this study contains 57.19% carbon. As shown in Equation 5, each kilogram of hydrochar can sequester approximately 2.097 kg of CO_2 emissions. However, to determine the net CO_2 sequestration, emissions from biomass processing, the hydrothermal liquefaction (HTL) process, and hydrochar drying must also be accounted for. According to Yang et al. [20], the hydrochar yield from HTL is 0.342, meaning that approximately 2.924 kg of biomass is required to produce 1 kg of hydrochar (Equation 6).

The energy consumption of the HTL process was also evaluated. Under laboratory conditions (at an ambient temperature of 25°C, a hydrolysis temperature of 270°C, and a reactor heating rate of 10°C per minute), it took 24.5 minutes to reach the hydrolysis temperature (Equations 7 and 8). The reactor (Parr 4580) then operated at 270°C for 20 minutes, consuming 60% of its nominal energy capacity during this period. Based on these parameters, the total energy consumption of the reactor for hydrochar and bio-oil production was estimated at 1.63 kWh (Equations 9 to 11).

Additional energy was required for drying. The oven, operating at 600 W, consumed 8.64 kWh to dry the biomass and 4.32 kWh to dry the hydrochar (Equations 12 and 13), considering the lower energy demand required to maintain the temperature. Consequently, the total energy demand for producing 1 kg of hydrochar was calculated as 14.59 kWh (Equation 14).

Based on Canada's national report [37], electricity production in Canada emits 0.1 kg of CO_2-eq per kWh. Thus, under laboratory conditions, the production of 1 kg of hydrochar is estimated to release 1.459 kg of CO_2-eq (Equation 15). It is important to note that scaling up production to an industrial level could significantly reduce energy consumption and, consequently, the associated CO_2 emissions. Ultimately, Equation 16 indicates that each kilogram of hydrochar has the potential to sequester at least 0.638 kg of CO_2-eq.

$$Saved\ CO_2 = \frac{Molar\ mass\ of\ CO_2 \times carbon\ content}{Molar\ mass\ of\ C} = \frac{44\frac{g}{mol} \times 571.9}{12\frac{g}{mol}} = 2.097\ kg\ CO_2 \tag{5}$$

$$Weight\ of\ biomass = \frac{Weight\ of\ hydrochar}{Yielding\ rate} = \frac{1\ kg}{0.342} = 2.924\ kg \tag{6}$$

$$Change\ in\ temperature = 270 - 25 = 245^o C \tag{7}$$

$$Required\ time\ for\ heating = \frac{Change\ in\ temperature}{Increasing\ rate} = \frac{245}{10} = 24.5\ min \tag{8}$$

$$E\ (heating\ phase) = power \times heating\ time = 2.8 \times \frac{25}{60} = 1.167\ kWh \tag{9}$$

$$E\ (holding\ phase) = efficiency \times power \times time = 0.5 \times 2.8 \times \frac{20}{60} = 0.467\ kWh \tag{10}$$

$$E_{hydrothermal} = E_{heat} + E_{hold} = 1.167 + 0.467 = 1.63\ kWh \tag{11}$$

$$E\ (oven\ biomass) = efficiency \times power \times\ time = 0.6 \times 0.6 \times 24 = 8.64\ kWh \tag{12}$$

$$E(oven\ hydrochar) = efficiency \times power \times time = 0.6 \times 0.6 \times 12 = 4.32\ kWh \tag{13}$$

$$E_{Total} = E_{hydro} + E_{oven\ biomass} + E_{oven\ hydrochar} = 1.63 + 8.64 + 4.32 = 14.59\ kWh \tag{14}$$

$$Required\ CO_2 - eq = 0.1 \frac{kg\ CO_2 - eq}{kWh} \times 14.59\ kWh = 1.459\ kg\ CO_2 - eq \tag{15}$$

$$Sequestered\ CO_2 = saved - required = 2.097 - 1.459 = 0.638\ kg\ CO_2 - eq \tag{16}$$

Since hydrothermal liquefaction at an industrial scale can be performed without drying the biomass, the energy required for hydrochar production could be reduced to 5.95 kWh. This would increase the sequestered carbon of hydrochar to 1.502 kg CO_2-eq per kilogram of hydrochar

(Equations 17 to 19). This might motivate the concrete industry to use hydrochar as a low-carbon solution for concrete.

$$E_{Total} = E_{hydro} + E_{oven\ hydrochar} = 1.63 + 4.32 = 5.95\ kWh \tag{17}$$

$$Required\ CO_2 - eq = 0.1 \frac{kg\ CO_2 - eq}{kWh} \times 5.95\ kWh = 0.595\ kg\ CO_2 - eq \tag{18}$$

$$Sequestered\ CO_2 = saved - required = 2.097 - 0.595 = 1.502\ kg\ CO_2 - eq \tag{19}$$

Table 7 presents the carbon footprint of the blended cement, calculated based on the dosage and CO_2-eq of its constituents, including OPC, slag, and silica fume. Table 8 displays the CO_2-eq of each mix component. Together with the quantities of each mix component required for manufacturing nine mortar cubes (50 × 50 × 50 mm^3) listed in Table 9, this data was used to estimate the CO_2-eq of each mix design, as shown in Table 10. Table 11 illustrates the scenario where hydrochar sequestration is considered to be 1.502 kg CO_2-eq per kilogram of hydrochar.

Table 7. CO_2 emissions of blended cement

Material	OPC	Slag	Silica fume	Blended cement
Carbon footprint (kg CO_2-eq/kg)	0.83 [38]	0.143 [39]	0.014 [40]	0.617

Table 8. Carbon footprint of the mix components

Material	Sand	Water	Blended cement	Hydrochar
Carbon footprint (kg CO_2-eq/kg)	0.0139 [10]	0 [10]	0.617	-0.638

The results indicate that incorporating hydrochar produced at an industrial scale, without drying the biomass, at a dosage of 0.5% could reduce the carbon footprint of conventional mortar by 1.15% in the additive series while having minimal impact on the compressive strength of the specimens. Increasing the hydrochar dosage to 2.5% could further reduce the carbon footprint of mortar by 8.09% and 5.73% in the SCM and additive series, respectively. Accordingly, hydrochar has the potential to serve as a low-carbon additive for cementitious composites, provided that challenges related to its disintegration and low strength are addressed.

Table 9. Quantity of mix components for 9 cubes

Mix design	Mix components (g)			
	Sand	Blended cement	Water	Hydrochar
Reference	2035	740	359	0
SCM-H0.5	2035	736.3	359	3.7
SCM-H1	2035	732.6	359	7.4
SCM-H2.5	2035	721.5	359	18.5
Add-H0.5	2035	740	359	3.7
Add-H1	2035	740	359	7.4
Add-H2.5	2035	740	359	18.5

Table 10. CO_2 emissions of each mix design (laboratory scale)

Mix design	CO_2-eq (g)				
	Sand	Blended cement	Water	Hydrochar	Total
Reference	28.287	456.580	0	0	484.867
SCM-H0.5	28.287	454.297	0	-2.361	480.223
SCM-H1	28.287	452.014	0	-4.721	475.580
SCM-H2.5	28.287	445.166	0	-11.803	461.65
Add-H0.5	28.287	456.58	0	-2.361	482.506
Add-H1	28.287	456.58	0	-4.721	480.146
Add-H2.5	28.287	456.58	0	-11.803	473.064

Table 11. CO_2 emissions of mixes considering industrial scale without preheating

Mix design	CO_2-eq (g)				
	Sand	Blended cement	Water	Hydrochar	Total
Reference	28.287	456.580	0	0	484.867
SCM-H0.5	28.287	454.297	0	-5.557	477.027
SCM-H1	28.287	452.014	0	-11.115	469.186
SCM-H2.5	28.287	445.166	0	-27.787	445.666
Add-H0.5	28.287	456.58	0	-5.557	479.31
Add-H1	28.287	456.58	0	-11.115	473.752
Add-H2.5	28.287	456.58	0	-27.787	457.080

6. Strengths and Limitations

This study analyzed the impact of hydrochar derived from HTL as both an SCM and an additive on the compressive strength, porosity, microstructure, and carbon footprint of cementitious composites. The findings provide valuable insights into how hydrochar influences both the macro- and micro-scale properties of these composites at 7, 28, and 90 days. Beyond the lab tests, this study also dives into key differences between hydrochar and biochar, as well as how hydrochar from HTC and HTL performs in mortar specimens.

Besides, there are limitations to consider. Since the experiments were carried out in a controlled lab environment, this study didn’t account for field curing conditions. This study primarily focused on the short-term properties of the mortars. Given the potential progress in hydrochar deterioration and its effect on the long-term properties of cementitious composites, the durability tests, particularly the acid and corrosion resistance of composites containing hydrochar, should be conducted in future studies.

Another limitation was the source and production procedure of hydrochar. The hydrochar's physicochemical properties depend on the type of biomass used and the production conditions, i.e., hydrothermal decomposition factors. Therefore, examining the effect of hydrochar derived from other biomass sources at different temperatures, durations, and pressures was necessary to fully understand and optimize its performance in cementitious composites. Addressing these gaps will enhance the applicability of the findings and support the broader adoption of hydrochar in construction practices.

7. Conclusions

This study examines the feasibility of incorporating hydrochar derived from the HTL of spent coffee grounds at 270°C and 20 bars for 20 minutes as both an SCM and an additive in cementitious mortars. The hydrochar from HTL had higher carbonization and fewer wooden organics than HTC's. This might improve its performance in the composites by raising their early-age strength and reducing their carbon footprint. Accordingly, 63 cubic specimens were prepared and cured in a standard moist curing chamber at a humidity level of 95–100%. The unit weight, ultrasonic pulse velocity, compressive strength, and microstructure of the specimens were analyzed at 7, 28, and 90 days to evaluate the performance of hydrochar in cementitious composites. An analysis of the carbon footprint was carried out to evaluate the environmental advantages of reusing hydrochar derived from HTL. The primary results of this study are listed below:

- The incorporation of hydrochar into the mortars at levels up to 2.5% consistently increased their porosity across all ages. The increased porosity was associated with a reduction in the unit weight (to 93.90, 95.75, and 96.00% for the SCM-Hx series and 93.76%, 95.24%, and 95.58% for the Add-Hx series at 7, 28, and 90 days, respectively, compared to the reference specimens) and ultrasonic pulse velocity (to 95.82, 96.21, and 95.41% for the SCM-Hx series and 94.34, 93.86, and 95.86% for the Add-Hx series at 7, 28, and 90 days, respectively, in comparison with the reference specimens).
- The effect of hydrochar on the compressive strength of mortars was highly time-dependent. While hydrochar significantly improved early-age strength, increasing CS by up to 19.24% and 9.57% in the SCM-Hx series and 59.59% and 44.02% in the Add-Hx series at 7 and 28 days, respectively, its long-term performance declined. Factors such as hydrochar's low reactivity, deterioration, disintegration, porosity, acidity, and the impact of accelerated

hydration reactions on the cement paste microstructure significantly reduced strength development between 28 and 90 days. As a result, the 90-day CS of specimens containing 2.5% hydrochar as an SCM and an additive decreased by 21.33% and 14.12%, respectively.

- Using hydrochar at 0.5% as an additive was the most efficient approach. It significantly improved the early-age strengths (by 59.59 and 44.02% at 7 and 28 days, respectively) and mitigated the carbon footprint of the mortars by 1.15% while having a minimal impact (about 0.1%) on the 90-day strength of the composite.
- Hydrochar improved the carbonization of the adjacent cement paste by releasing functional groups from its shells during dissolution, resulting in a reduction in the shell's carbon percentage from 57.19 to a range of 44 to 33.8%. Although the carbonization could strengthen the cement paste, the dissolution resulted in hydrochar deterioration and disintegration, increasing the porosity and reducing the CS of the system.
- Hydrochar's disintegration, deterioration, acidity, and shrinkage in cement paste underscore the presence of wooden organics within these particles. This observation indicates the necessity for additional preprocessing techniques before hydrothermal decomposition, which can improve the chemical stability of the particles and ensure a uniform distribution of chemical compositions throughout them.
- The hydrochar enhanced the strength of cementitious composites by supplying additional water, providing nucleation sites, offering dissolved carbon, and refining the size of pores in cement paste. Nonetheless, its physical morphology, shrinkage, deterioration, low pH, and tendency to accelerate hydration reactions, which could lead to microcrack formation, ultimately weakened its interfacial transition zone with cement paste over time, offsetting its initial benefits..

- Hydrochar's impact on the cementitious composites, particularly their strengthening reactions over various intervals, substantially relied on the hydrothermal parameters, including temperature, duration, and pressure, as well as the source of the biomass. This is because the factors affect the chemical stability, porosity, water absorption capacity, and quantity of wooden organics in the hydrochar particles.
- HTL-derived hydrochar can sequester up to 1.502 kg CO_2-eq per kilogram, offering a promising sustainable alternative to cement for reducing the carbon footprint of cementitious composites. Incorporating hydrochar at dosages up to 2.5% (by cement weight) could reduce mortar-related CO_2 emissions by up to 8.9%, further supporting its potential as an environmentally friendly material.
- Precise models were developed to estimate the 90-day unit weight, ultrasonic pulse velocity, and compressive strength of the composite containing hydrochar when the hydrochar dosage changes in the range of 0 to 2.5% with respect to the weight of cement.

This study illustrated the efficacy of hydrochar from hydrothermal liquefaction as both an additive and a supplementary cementitious material in cementitious composites. The findings indicated that the composite incorporating hydrochar exceeded the minimum standards for mortars, thereby promoting environmental sustainability and facilitating the acceleration of construction projects. The research suggested incorporating 0.5% hydrochar as an additive in cementitious composites, as it could markedly enhance early-age strength without compromising long-term strength. Given the carbon sequestration feature of hydrochar, it could be considered a low-carbon solution for cementitious composites, while its incorporation could significantly benefit the construction industry by reducing the waiting time for concrete strengthening. However, the durability of the hydrochar-modified composites should be examined prior to their adoption into the industry.

Future Studies

The findings underscored the significance of hydrothermal preprocessing and durability assessments. The incorporation of hydrochar enhanced the strength of the specimens at 7 and 28 days; however, its deterioration, disintegration, shrinkage, and acidity negatively impacted the composites' strength at 90 days. The hydrothermal modification, such as increasing hydrothermal time, temperature, and pressure, and grinding the biomass prior to HTL may improve the chemical stability of hydrochar particles and diminish variations in their chemical compositions. The increased carbonization could also reduce the wooden organics and functional groups in the hydrochar. This approach can decrease the shrinkage and deterioration rates and avoid disintegration of the particles, thereby mitigating their negative effects on the long-term properties of the composite.

Increased exposure of hydrochar to cement paste can also reduce the compressive strength of the composites by elevating the levels of hydrochar deterioration and disintegration. Besides, the low pH of hydrochar may cause acid production in its vicinity, leading to the dissolution of hydration products adjacent to the particles. This may result in raised porosity of the composites, consequently decreasing their strength. These underscore the significance of durability studies in assessing the long-term performance of hydrochar-modified composites particularly its permeability and resistance against chemical attacks such as sulfate and chloride attack.

Despite the adverse effects of hydrochar on long-term compressive strength, which may discourage researchers from utilizing it as an SCM and an additive in cementitious composites, the findings could pave the way for exploring its role as recycled aggregates. A small dosage of hydrochar can significantly accelerate the construction of concrete elements by promoting early-age strengthening and reducing CO_2 emissions through its carbon sequestration capability.

Acknowledgments

The authors would like to thank Dr. Quan (Sophia) He and Dr. Himadri Rajput from the Department of Engineering, Faculty of Agriculture at Dalhousie University for providing hydrochar for the study. The authors would also like to express their gratitude to the staff of Dalhousie University's structural and concrete lab, as well as Dr. Ping Li from the Department of Biology and Dr. Eric Moreau from the Department of Mechanical Engineering, for their cooperation during the testing. Financial support from the Nova Scotia Graduate Scholarship and Canada Research Chair programs is acknowledged.

References

[1] L. Proaño, A.T. Sarmiento, M. Figueredo, M. Cobo, Techno-economic evaluation of indirect carbonation for CO2 emissions capture in cement industry: A system dynamics approach, J Clean Prod 263 (2020) 121457. https://doi.org/10.1016/j.jclepro.2020.121457.

[2] United Nations Environment Programme, 2022 Global Status Report for Buildings and Construction: Towards a Zero-emission, Efficient and Resilient Buildings and Construction Sector, Nairobi, 2022. https://www.unep.org/resources/publication/2022-global-status-report-buildings-and-construction (accessed January 21, 2025).

[3] N. Dave, A.K. Misra, A. Srivastava, A.K. Sharma, S.K. Kaushik, Study on quaternary concrete micro-structure, strength, durability considering the influence of multi-factors, Constr Build Mater 139 (2017) 447–457. https://doi.org/10.1016/j.conbuildmat.2017.02.068.

[4] A. Jafari, P. Sadeghian, Applications of Recycled Gypsum from Waste Drywalls in the Construction Industry: A Review, in: Proceedings of the Canadian Society of Civil Engineering Annual Conference 2022, Springer, 2024: pp. 817–832. https://doi.org/10.1007/978-3-031-34027-7_54.

[5] A.M. Rashad, S.R. Zeedan, The effect of activator concentration on the residual strength of alkali-activated fly ash pastes subjected to thermal load, Constr Build Mater 25 (2011) 3098–3107. https://doi.org/10.1016/j.conbuildmat.2010.12.044.

[6] O. Bourzik, N. Akkouri, K. Baba, A. Nounah, Study of the effect of wood waste powder on the properties of concrete, Mater Today Proc 58 (2022) 1459–1463. https://doi.org/10.1016/j.matpr.2022.02.518.

[7] D. Baturkin, O.A. Hisseine, R. Masmoudi, A. Tagnit-Hamou, L. Massicotte, Valorization of recycled FRP materials from wind turbine blades in concrete, Resour Conserv Recycl 174 (2021) 105807. https://doi.org/10.1016/j.resconrec.2021.105807.

[8] J. Hu, H. Guo, X. Wang, M. Gao, G. Yao, Y.F. Tsang, J. Li, J. Yan, S. Zhang, Utilization of the saccharification residue of rice straw in the preparation of biochar is a novel strategy for reducing CO2 emissions, Science of The Total Environment 650 (2019) 1141–1148. https://doi.org/10.1016/j.scitotenv.2018.09.099.

[9] A. Jafari, P. Sadeghian, Effect of Biochar from Waste Wood on the Strength of Cementitious Mortar: Additive and Cement Replacement, in: Proceedings of the Canadian Society for Civil Engineering Annual Conference 2023, Springer, 2025: pp. 227–238. https://doi.org/10.1007/978-3-031-61507-8_19.

[10] A. Jafari, P. Sadeghian, Biochar and recycled gypsum drywall in concrete: role and effects on compressive behavior, microstructure, and carbon footprint, J Sustain Cem Based Mater 14 (2025) 119–144. https://doi.org/10.1080/21650373.2024.2428987.

[11] S. Barbhuiya, B. Bhusan Das, F. Kanavaris, Biochar-concrete: A comprehensive review of properties, production and sustainability, Case Studies in Construction Materials 20 (2024) e02859. https://doi.org/10.1016/j.cscm.2024.e02859.

[12] A. Belaadi, M. Boumaaza, H. Alshahrani, M. Bourchak, Optimization of Palm Rachis Biochar Waste Content and Temperature Effects on Predicting Bio-Mortar : ANN and RSM Modelling, Journal of Natural Fibers 20 (2023). https://doi.org/10.1080/15440478.2022.2151547.

[13] W. Xu, Y. Zhang, M. Li, F. Qu, C.S. Poon, X. Zhu, D.C.W. Tsang, Durability and micromechanical properties of biochar in biochar-cement composites under marine environment, J Clean Prod 450 (2024) 141842. https://doi.org/10.1016/j.jclepro.2024.141842.

[14] H.A. Ruiz, M. Galbe, G. Garrote, D.M. Ramirez-Gutierrez, E. Ximenes, S.-N. Sun, D. Lachos-Perez, R.M. Rodríguez-Jasso, R.-C. Sun, B. Yang, M.R. Ladisch, Severity factor kinetic model as a strategic parameter of hydrothermal processing (steam explosion and liquid hot water) for biomass fractionation under biorefinery concept, Bioresour Technol 342 (2021) 125961. https://doi.org/10.1016/j.biortech.2021.125961.

[15] D. Lachos-Perez, P. César Torres-Mayanga, E.R. Abaide, G.L. Zabot, F. De Castilhos, Hydrothermal carbonization and Liquefaction: differences, progress, challenges, and opportunities, Bioresour Technol 343 (2022) 126084. https://doi.org/10.1016/j.biortech.2021.126084.

[16] Y.H. Chan, R.R. Tan, S. Yusup, H.L. Lam, A.T. Quitain, Comparative life cycle assessment (LCA) of bio-oil production from fast pyrolysis and hydrothermal liquefaction of oil palm empty fruit bunch (EFB), Clean Technol Environ Policy 18 (2016) 1759–1768. https://doi.org/10.1007/s10098-016-1172-5.

[17] M.M. Santos, A.L. Marques Sierra, Á. Amado-Fierro, M. Suárez, F. Blanco, J.M.G. La Fuente, M.A. Diez, T.A. Centeno, Reducing cement consumption in mortars by waste-derived hydrochars, Journal of Building Engineering 75 (2023) 106987. https://doi.org/10.1016/j.jobe.2023.106987.

[18] M. Sharma, İ.Ş. Öztürk, M. Emiroğlu, A.S. Erses Yay, Performance evaluation of biomass-derived hydrothermal carbonaceous material in cement based composites, Case Studies in Construction Materials 22 (2025) e04291. https://doi.org/10.1016/j.cscm.2025.e04291.

[19] A. Jafari, P. Sadeghian, Influence of biochar and recycled gypsum on the strength and microstructure of conventional and sustainable cementitious composites, Constr Build Mater 408 (2023) 133715. https://doi.org/10.1016/j.conbuildmat.2023.133715.

[20] J. Yang, Z. Zhao, Y. Hu, Lord Abbey, I. Cesarino, A. Goonetilleke, Q. He, Exploring the Properties and Potential Uses of Biocarbon from Spent Coffee Grounds: A Comparative Look at Dry and Wet Processing Methods, Processes 11 (2023) 2099. https://doi.org/10.3390/pr11072099.

[21] Y. Hu, R. Gallant, S. Salaudeen, A.A. Farooque, S. He, Hydrothermal Carbonization of Spent Coffee Grounds for Producing Solid Fuel, Sustainability 14 (2022) 8818. https://doi.org/10.3390/su14148818.

[22] R. Roychand, S. Kilmartin-Lynch, M. Saberian, J. Li, G. Zhang, C.Q. Li, Transforming spent coffee grounds into a valuable resource for the enhancement of concrete strength, J Clean Prod 419 (2023) 138205. https://doi.org/10.1016/j.jclepro.2023.138205.

[23] L. Qing, H. Zhang, Z. Zhang, Effect of biochar on compressive strength and fracture performance of concrete, Journal of Building Engineering 78 (2023) 107587. https://doi.org/10.1016/j.jobe.2023.107587.

[24] G. Murali, L.S. Wong, A comprehensive review of biochar-modified concrete: Mechanical performance and microstructural insights, Constr Build Mater 425 (2024) 135986. https://doi.org/10.1016/j.conbuildmat.2024.135986.

[25] Z. Cao, S. Zhang, X. Huang, H. Liu, M. Sun, J. Lyu, Correlations between the compressive strength of the hydrochar pellets and the chemical components: Evolution and densification mechanism, J Anal Appl Pyrolysis 152 (2020) 104956. https://doi.org/10.1016/j.jaap.2020.104956.

[26] American Society for Testing and Materials, ASTM C109/109M-21: Standard Test Method for Compressive Strength of Hydraulic Cement Mortars (Using 2-in. or [50 mm] Cube Specimens), ASTM, 2021.

[27] T. Gutberlet, H. Hilbig, R.E. Beddoe, Acid attack on hydrated cement — Effect of mineral acids on the degradation process, Cem Concr Res 74 (2015) 35–43. https://doi.org/10.1016/j.cemconres.2015.03.011.

[28] J. Wang, G. Long, Y. Xiang, R. Dong, Z. Tang, Q. Xiao, Z. Yang, K. Ma, Influence of rapid curing methods on concrete microstructure and properties: A review, Case Studies in Construction Materials 17 (2022) e01600. https://doi.org/10.1016/j.cscm.2022.e01600.

[29] M. Li, X. Zhu, Y. Zhang, D.C.W. Tsang, A multi-phase mechanical model of biochar–cement composites at the mesoscale, Computer-Aided Civil and Infrastructure Engineering (2024). https://doi.org/10.1111/mice.13307.

[30] X. Zhu, Y. Zhang, L. Chen, L. Wang, B. Ma, J. Li, C.S. Poon, D.C.W. Tsang, Bonding mechanisms and micro-mechanical properties of the interfacial transition zone (ITZ) between biochar and paste in carbon-sink cement-based composites, Cem Concr Compos 139 (2023) 105004. https://doi.org/10.1016/j.cemconcomp.2023.105004.

[31] R.B.W. Evaristo, R. Ferreira, J. Petrocchi Rodrigues, J. Sabino Rodrigues, G.F. Ghesti, E.A. Silveira, M. Costa, Multiparameter-analysis of CO2/Steam-enhanced gasification and pyrolysis for syngas and biochar production from low-cost feedstock, Energy Conversion and Management: X 12 (2021) 100138. https://doi.org/10.1016/j.ecmx.2021.100138.

[32] G. Mishra, P.A. Danoglidis, S.P. Shah, M.S. Konsta-Gdoutos, Carbon capture and storage potential of biochar-enriched cementitious systems, Cem Concr Compos 140 (2023) 105078. https://doi.org/10.1016/j.cemconcomp.2023.105078.

[33] R.B. Fidel, D.A. Laird, M.L. Thompson, M. Lawrinenko, Characterization and quantification of biochar alkalinity, Chemosphere 167 (2017) 367–373. https://doi.org/10.1016/j.chemosphere.2016.09.151.

[34] J. Lehmann, M.C. Rillig, J. Thies, C.A. Masiello, W.C. Hockaday, D. Crowley, Biochar effects on soil biota – A review, Soil Biol Biochem 43 (2011) 1812–1836. https://doi.org/10.1016/j.soilbio.2011.04.022.

[35] J.-H. Yuan, R.-K. Xu, H. Zhang, The forms of alkalis in the biochar produced from crop residues at different temperatures, Bioresour Technol 102 (2011) 3488–3497. https://doi.org/10.1016/j.biortech.2010.11.018.

[36] S. Gupta, A. Kashani, Utilization of biochar from unwashed peanut shell in cementitious building materials – Effect on early age properties and environmental benefits, Fuel Processing Technology 218 (2021) 106841. https://doi.org/10.1016/j.fuproc.2021.106841.

[37] L. Pratt, NATIONAL INVENTORY REPORT 1990 –2021: GREENHOUSE GAS SOURCES AND SINKS IN CANADA, Gatineau, 2023. https://publications.gc.ca/collections/collection_2023/eccc/En81-4-2021-1-eng.pdf (accessed February 11, 2025).

[38] A. Adesina, Recent advances in the concrete industry to reduce its carbon dioxide emissions, Environmental Challenges 1 (2020) 100004. https://doi.org/10.1016/j.envc.2020.100004.

[39] A. Jafari, V. Toufigh, Developing a comprehensive prediction model for the compressive strength of slag-based alkali-activated concrete, J Sustain Cem Based Mater (2023) 1–18. https://doi.org/10.1080/21650373.2023.2266442.

[40] G.P. Hammond, C.I. Jones, Embodied energy and carbon in construction materials, Proceedings of the Institution of Civil Engineers - Energy 161 (2008) 87–98. https://doi.org/10.1680/ener.2008.161.2.87.